IAC TECHNOLOGY DIVISION

IP/UM-OSI/564v.3

IPUMOSI_564V3.DOC

March 14, 2012

Project Ref.:

PROJECT / DESTINATION:

OSIRIS

TITLE:

TF USER MANUAL

INSTITUTO DE ASTROFISICA DE CANARIAS

38200 La Laguna (Tenerife) - ESPAÑA - Phone (922)605200 - Fax (922)605210

AUTHOR LIST

Name	Function
Jordi Cepa	OSIRIS Principal Investigator

APPROVAL CONTROL

Control	Name	Function
Revised by:		
Approved by:		
Authorised by:		

DOCUMENT CHANGE RECORD

Issue	Date	Change Description
1	28/06/09	First version
2	18/01/11	Changes on section 4.4
3	14/03/12	New TF calibration (section 4.4)

SUMMARY

This document provides a general description of the basics concepts about Tunable Filters, plus brief and simple practical instructions for designing TF observations for different types of targets, and scientific cases, and for calibrating and operating OSIRIS Tunable Filters. As instrument commissioning and operation progresses, it is expected that this document, that complements the OSIRIS user manual, will be updated accordingly.

The section on charge shuffling and fast modes is still pending.

TABLE OF CONTENTS

AUTHOR LIST **2**

APPROVAL CONTROL **2**

DOCUMENT CHANGE RECORD **2**

SUMMARY **3**

TABLE OF CONTENTS **4**

LIST OF ABBREVIATIONS **7**

1. INTRODUCTION **8**

1.1 SCOPE 8
1.2 CONTACT INFORMATION 8

2. TUNABLE FILTERS **8**

2.1 TF CONCEPT 8
2.2 INTRODUCTION TO FABRY-PEROT FILTERS (FPFS) 8
2.2.1 Performance of an ideal FPF *9*
2.2.2 Limitations *11*
2.2.3 Gap-scanning etalons *12*
2.2.4 Piezo-electric transducers *13*
2.2.5 Capacitance micrometry *14*
2.3 CHARGE SHUFFLING 14
2.4 ORDER SORTERS 14

3. TUNABLE IMAGING VERSUS SPECTROSCOPY **14**

4. OSIRIS TF CHARACTERISTICS AND FEATURES **16**

4.1 GENERAL 16
4.2 DIMENSIONS 17
4.3 COATINGS 17
4.4 WAVELENGTH VARIATION ACROSS THE FOV 18
4.5 GHOSTS 22
4.6 CALIBRATIONS REQUIRED 23
4.6.1 Paralellism calibration *23*
4.6.2 Wavelength calibration *24*
4.7 TUNING ACCURACY 25
4.8 TUNING SPEED 25
4.9 TUNING RANGE 25
4.10 OSIRIS TF FOV 26

5. OBSERVING STRATEGIES **26**

5.1 SELECTING OFF BAND 27
5.1.1 Continuum subtraction *27*

5.1.2 Off-band wavelength and FWHM tuning selection 27
5.2 DEBLENDING LINES 28
5.3 ON-LINE FWHM SELECTION 29
5.4 DECIDING TARGET POSITION AND ORIENTATION 30
5.5 REMOVING GHOSTS, COSMIC RAYS AND COSMETICS 31
5.5.1 Half field masking 31
5.5.2 Azimuthal dithering pattern 31
5.5.3 TF tuning dithering pattern 32
5.6 TUNABLE TOMOGRAPHY 32
5.6.1 Technique 32
5.6.2 Some applications 33
5.7 BAND SYNTHESIS TECHNIQUE 33
5.7.1 Technique 33
5.7.2 Some applications 34
5.8 SOURCES OF INSTRUMENTAL PHOTOMETRIC ERRORS. SUMMARY 34

6. STARTING UP OSIRIS TF 35

7. CALIBRATING OSIRIS TF 36

7.1 PARALLELISM 36
7.1.1 General considerations 36
7.1.2 OSIRIS TF parallelization procedure 36
7.1.3 Lack of parallelism 45
7.1.4 Troubleshooting 46
7.1.4.1 The X or Y Sweep does not stop 46
7.1.4.2 The X, Y or Z give very different values in consecutive exposures or even mirrored rings 46
7.2 WAVELENGTH CALIBRATION 47
7.2.1 General considerations 47
7.2.2 Calibration using the ICM 48
7.2.3 Calibration using astronomical targets 48
7.2.4 Calibration using sky rings 49
7.2.5 Trade-offs 51
7.2.6 Measuring TF FWHM 51
7.3 FLUX CALIBRATION 51

8. OPERATING OSIRIS TF 52

8.1 TF SETUP 52
8.2 STANDARD EXPOSURES 52
8.3 SHUFFLED EXPOSURES 55
8.4 FAST MODES 55
8.4.1 Charge shuffling 56
8.4.2 Frame transfer 56

9. OBSERVING WITH OSIRIS TF 56

9.1 GENERAL PROCEDURE 56
9.1.1 Preparing observation 56
9.1.2 Day time routines 57
9.1.3 Practical TF operation and calibrations during the night 57

10. POST-PROCESSING TF DATA 58

10.1 GENERAL CONSIDERATIONS 58
10.2 CALIBRATION IMAGES 59
10.2.1 Bias *59*
10.2.2 Flatfields *59*
10.3 SKY RINGS 59

11. POWERING DOWN 60

12. TROUBLESHOOTING 60

12.1 LCU FREEZES 60
12.2 TF CANNOT BE SHUTDOWN 60
12.3 TF DO NOT STARTUP 61

ANNEXES 62

A. REFERENCES 62

B. OSIRIS ORDER SORTERS 63

B.1. RED ETALON OSS 63
B.2. BLUE ETALON OSS 64

C. OSIRIS TF WAVELENGTH CALIBRATORS 65

C.1. SELECTED ARC LINES 66
C.2. SELECTED COMPACT PLANETARY NEBULAE 67
C.3. SELECTED BRIGHT TYPE II QSO 68

D. SELECTED STANDARDS FOR FLUX CALIBRATION 70

E. SOME USEFUL FORMS 71

E.1. FOR KEEPING TRACK OF PARALLELISMS AND Z OFFSETS 71

LIST OF ABBREVIATIONS

AC	Altern Current
CCCS	Control Cabinet Control System
CCD	Charge Coupled Device
DAS	Data Acquisition System
FSR	Free Spectral Range
FWHM	Full Width Half Maximum
GCS	GTC Control System
GTC	Gran Telescopio Canarias
HV	High Voltage
ICM	Instrument Calibration Module
IPA	Instrument Position Angle
LCU	Local Control Unit
MAD	Módulo de Arranque Distribuido
MCS	Main Control System
MOC	Módulo Comunicaciones
OB	Observing Block
OSIRIS	Optical System for Imaging and low Resolution Integrated Spectroscopy
OS	Order Sorter
PN	Planetary Nebula
QSO	Quasi Stellar Object
SA	Support Astronomer
SDSS	Sloan Digital Sky Survey
SDSU	San Diego State University
S/N	Signal-to-noise ratio
STIS	Space Telescope Imaging Spectrograph
TBC	To Be Confirmed
TBD	To Be Defined
TF	Tunable Filter

1. INTRODUCTION

1.1 Scope

This document is aimed at providing the:

1. Users with the basic information required for designing a successful observation of their favourite targets using OSIRIS TFs

2. GTC SAs with the basic information required for start up, initialize, configure, use, calibrate, and power off the OSIRIS TFs. Some troubleshooting basics is provided as well.

IMPORTANT NOTE: It is advisable that TF are always operated by GTC SAs or by OSIRIS Instrument Team members only, not by visiting astronomers, regardless of their experience in etalons.

1.2 Contact information

The information presented here can be found in the form of slides in the OSIRIS WWW http://www.iac.es/project/OSIRIS. The calculators can be found in the same page as well.

For specific or further queries, please contact OSIRIS PI at jcn@iac.es.

2. TUNABLE FILTERS

2.1 TF concept

A key aspect of OSIRIS is the use of tunable filters (TFs). OSIRIS TFs are a pair of tunable narrow-band interference filters (Fabry-Perot etalons) covering 370–670 nm (blue 'arm') and 650–960 nm (red 'arm'). They offer monochromatic imaging with an adjustable passband of between 0.6 and 3 nm. In addition, TF frequency switching can be synchronized with movement of charge (charge shuffling or frame transfer) on the OSIRIS CCDs, techniques that have important applications to many astrophysical problems.

2.2 Introduction to Fabry-Perot filters (FPFs)

In its simplest form, a Fabry-Perot filter (FPF) consists of two plane parallel transparent plates which are coated with films of high reflectivity and low absorption. The coated surfaces are separated by a small distance (typically μm to mm) to form a cavity which is resonant at specific wavelengths. Light entering the cavity undergoes multiple reflections (Figure 2.1) with the amplitude and phase of the resultant beams depending on the wavelength. At the resonant wavelengths, the resultant reflected beam interferes constructively with the light reflected from the first plate-cavity boundary and all the incident

energy, in the absence of absorption, is transmitted. At other wavelengths, the FPF reflects almost all of the incident energy.

2.2.1 Performance of an ideal FPF

The general equation for the intensity transmission coefficient of an ideal FPF (perfectly flat plates used in a parallel beam) as a function of wavelength is

$$\tau_r = \left(\frac{T}{1-R}\right)^2 \left[1 + \frac{4R}{(1-R)^2} sin^2\left(\frac{2\pi\mu d\cos\theta}{\lambda}\right)\right]^{-1}, \quad (2.1)$$

where T is the transmission coefficient of each coating (plate–cavity boundary), R is the reflection coefficient , d is the plate separation, μ is the refractive index of the medium in the cavity (usually air, μ =1) and θ is the angle of incident light. Thus, the FPF transmits a narrow spectral band at a series of wavelengths given by

$$m\lambda = 2\mu d\cos\theta \quad (2.2)$$

where m is an integer known as the order of interference. The peak transmission of each passband is

$$\tau_{r,max} = \left(\frac{T}{1-R}\right)^2 = \left(\frac{T}{T+A}\right)^2, \quad (2.3)$$

where A is the absorption and scattering coefficient of the coatings ($A = 1 - T - R$); and the minimum transmission, halfway between the resonant wavelengths is

Therefore, the contrast between the maximum and minimum transmission intensities is

$$C_r = \frac{\tau_{r,max}}{\tau_{r,min}} = \left(\frac{1+R}{1-R}\right)^2. \quad (2.4)$$

For a FPF contrast greater than 100, the reflection coefficient R of the coatings needs to be greater than or about 0.82.

The wavelenght spacing between passbands, known as the inter–order spacing or free spectral range (FSR), is about

$$\Delta\lambda = \frac{\lambda}{m} \quad (2.5)$$

which is obtained from Equation 2.2 by setting consecutive integral values of m. Each passband has a bandwidth ($\delta\lambda$), full width at half-peak transmission, given by

$$\delta\lambda_r = \frac{\lambda(1-R)}{m\pi R^{1/2}} \quad (2.6)$$

derived from Equation 2.1. The ratio of inter–order spacing to bandwidth is called the finesse;

$$N = \frac{\Delta\lambda}{\delta\lambda}. \tag{2.7}$$

$$\tau_{r,min} = \left(\frac{T}{1+R}\right)^2. \tag{2.8}$$

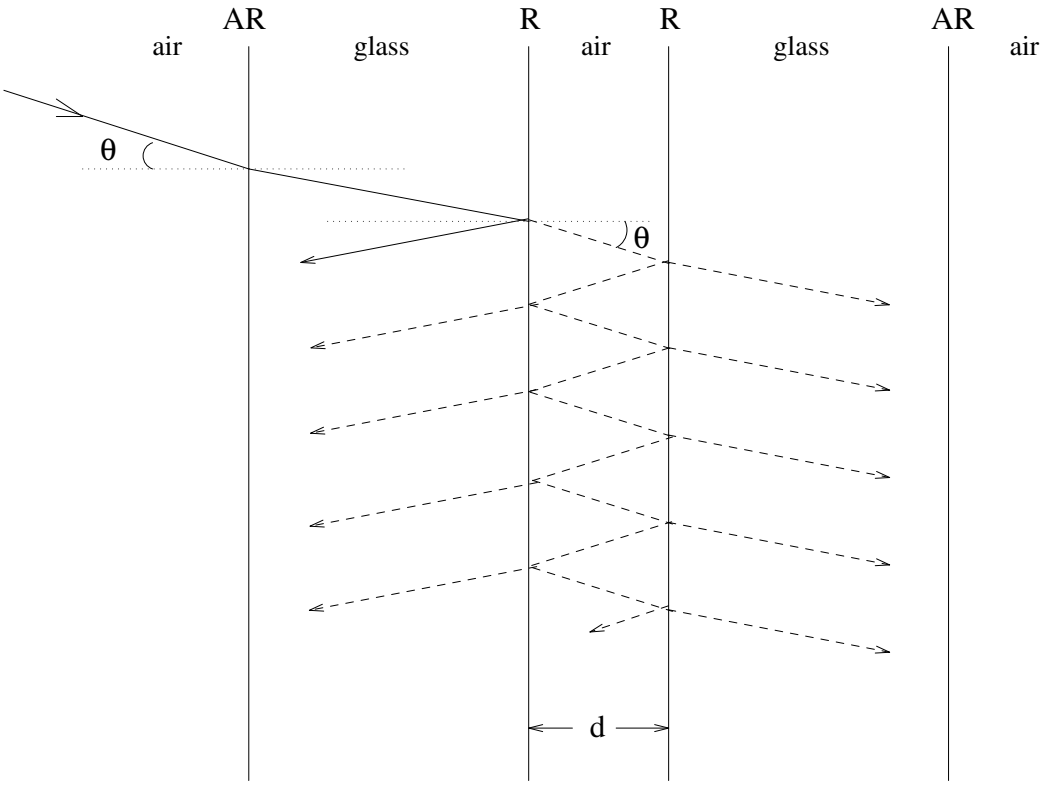

Figure 2.1 Schematic diagram of interference with a Fabry-Perot filter. The outside surfaces of the glass are coated with anti-reflective (AR) coatings, while the inside surfaces are highly reflective (usually $R > 0.8$). The air cavity in the middle is not shown to scale (usually, d is about 10 μm whereas the glass is over 20 mm thick on both sides). At resonant wavelengths, the first reflection (shown with a solid line) interferes destructively with light coming from the cavity in the same direction (dashed lines). The phase difference arises because the first reflection is `internal', while all the other reflections are `external' (with respect to glass). On the other side of the cavity, only constructive interference occurs. At non-resonant wavelengths, destructive interference occurs in the cavity and the first reflection dominates.

For an ideal FPF, it is given by

$$N_r = \frac{\Delta\lambda}{\delta\lambda_r} = \frac{\pi R^{1/2}}{1-R}. \tag{2.9}$$

Thus, we can see that the resolving power of a FPF is equal to the product of the order and the finesse;

$$\frac{\lambda}{\delta\lambda} = mN. \tag{2.10}$$

2.2.2 Limitations

It is apparent from the above equations that to obtain a higher resolution for a given order or to obtain a wider inter-order spacing for a given resolution, the finesse needs to be increased. For a finesse greater than 100, a reflection coefficient R of greater than or about 0.97 is necessary (Equation 2.9). However, so far we have considered the ideal situation where the plates are flat and parallel, and the incoming light is parallel. In particular, Equations 2.1, 2.3–2.5, 2.7 and 2.9 refer to this situation using the subscript r to distinguish the results from a real filter. In practice, plate defects and the angular size of the beam limit the maximum finesse obtainable.

The effective finesse (N) is approximately given by

$$\frac{1}{N^2} = \frac{1}{N_r^2} + \frac{1}{N_d^2} + \frac{1}{N_a^2}, \tag{2.11}$$

where N_r is the reflective finesse from Equation 2.33, N_d is the defect finesse (due to plate defects) and N_a is the aperture finesse (due to the solid angle of the beam).

The defect finesse

$$N_d \sim \frac{2\pi}{2\delta d}, \tag{2.12}$$

where δd is a length scale related to deviations from flat parallel plates. The exact details depend on the type of deviations (Atherton et al. 1981). A FPF manufactured with $N_d \sim 80$ and a reflection coefficient of 0.97 ($N_r \sim 100$) performs with a finesse of about 60.

The aperture finesse

$$N_a \sim \frac{2\pi}{m\Omega}, \tag{2.13}$$

where Ω is the solid angle of the cone of rays passing through the FPF. This equation is related to the λ dependence on θ in Equation 2.2. In terms of astronomical imaging, the effect of aperture finesse is negligible for most objects in the field of view of a telescope. For example, an object which is one degree across (in the collimated beam) imaged with m =50 has N_a ~500 according to Equation 2.13. A more relevant analysis to consider the change in central wavelength of the filter as the ray angle θ is varied in Equation 2.2. For example, a change in ray angle from 1° to 3° produces a change of 0.1% in the central wavelength of the

filter at any given order. Therefore, at high resolving powers (~1000), a FPF may not be truly monochromatic across a desired field of view.

2.2.3 Gap-scanning etalons

In order to manufacture a tunable FPF, which can change the central wavelength for a given order, it is necessary to be able to adjust either the refractive index of the cavity μ, the plate separation d or the angle θ (as can clearly be seen from Equation 2.2). In a gap-scanning etalon, the plate separation can be controlled to extremely high accuracy.

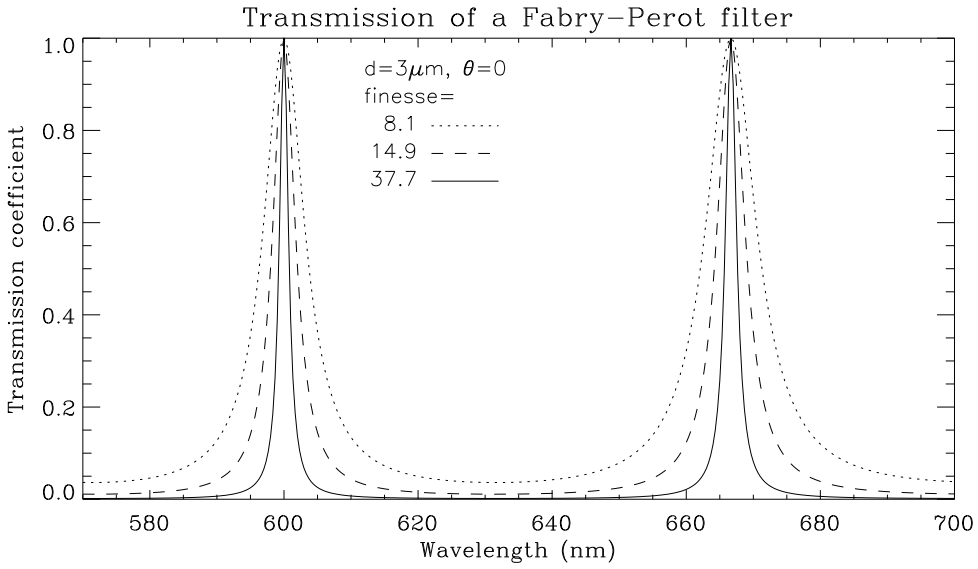

Figure 2.2 Variation of the transmission profile of a FPF with finesse. The profiles were determined for an ideal FPF (Equation 2.25) with R = 0.68, 0.81 and 0.92 (A = 0). Orders m = 10 and m = 9 are shown.

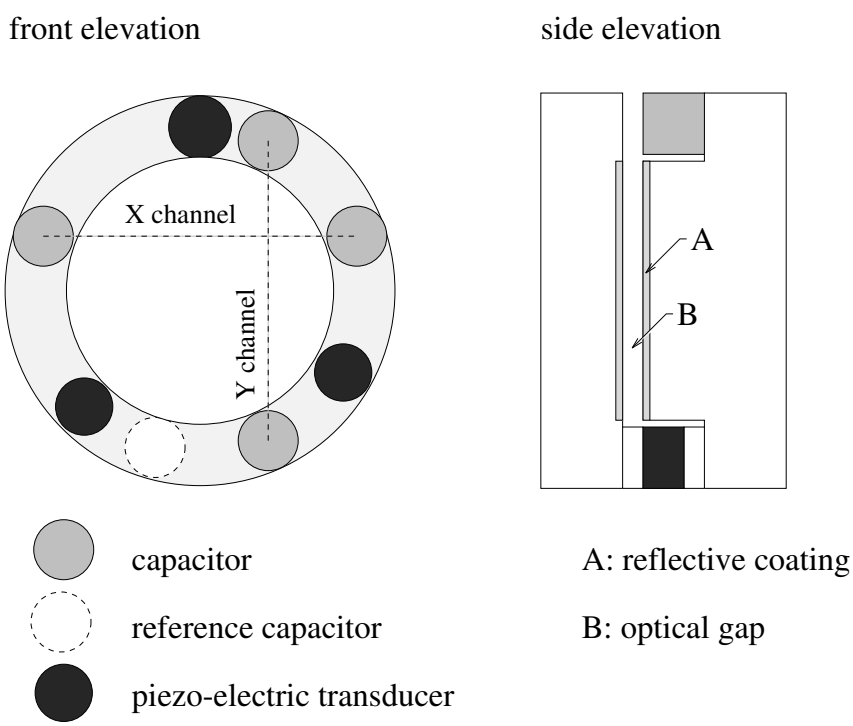

Figure 2.3 Front elevation and side elevation of a *Queensgate Instruments* etalon. Note that the thickness of the optical gap is exaggerated.

In Figure 2.3, we show the structure of a gap-scanning etalon manufactured by *Queensgate Instruments Ltd.* (now *IC Optical Systems*) In recent years, these etalons have undergone considerable improvements. It is now possible to move the plates between any two discrete spacings at very high frequencies (200 Hz or better) with no hysteresis effects while maintaining λ/2000 parallelism (measured at 633 nm). The etalon spacing is maintained by three piezo-electric transducers as discussed below.

2.2.4 Piezo-electric transducers

Piezo-electric materials undergo dimensional changes in an applied electric field. Conversely, they develop an electric field when strained mechanically. Under an applied electric field, a piezoelectric crystal deforms along all its axes. It expands in some directions and contracts in others. The dimensional change (expansion or contraction) of a piezo-electric material is a smooth function of the applied electric field. The material is sufficiently stiff that piezo-electric transducers (PZTs) can respond on sub-microsecond time scales (Atherton 1995). The resolution is limited only by the precision with which the electric field can be controlled. For this reason, PZTs are commonly used for rapid switching and sensing, as indeed they are in the *Queensgate* etalons. However, all piezo-electric materials exhibit hysteresis, particularly in the relationship between the voltage applied and the amount of expansion. Thus, a servo-control system is required to tune the spacing between two plates to high accuracy.

2.2.5 Capacitance micrometry

In a seminal paper, Jones & Richards (1973) show that capacitance micrometry can be used to detect motions on scales as small as 10^{-15}m. Using this basic method, *Queensgate Instruments* have developed a capacitance bridge system to monitor parallelism and spacing of a Fabry-Perot etalon (Hicks et al. 1984). Information from the capacitance bridge is used to drive PZTs in a closed loop control system to maintain the parallelism and spacing. In Figure 3, we show the basic structure of a gap-scanning etalon. There are two x-channel and two y-channel capacitors, and a fifth 'reference' capacitor which monitors the spacing with respect to a fixed reference capacitor in the circuit. The two etalon plates can be kept parallel with an accuracy of $\lambda/200$ for many weeks at a time.

2.3 Charge shuffling

Central to almost all modes of OSIRIS use is charge shuffling. Charge shuffling is movement of charge along the CCD between multiple exposures of the same frame, before the image is read out. For shuffled TF imaging an aperture mask ensures that only a section of the CCD frame is exposed at a time. For each exposure, the tunable filter is systematically moved to different gap spacings in a process called frequency-switching. This way, a region of sky can be captured at several different wavelengths on a single image. Alternatively, the TF can be kept at fixed frequency and charge shuffling performed to produce time-series exposures.

The TF plates can be switched anywhere over the physical range at rates in excess of 100 Hz, although in most applications, these rates rarely exceed 0.1 Hz. If a shutter is used, this limits the switching rate to about 1 Hz. Charge on OSIRIS CCDs can be moved over the full area at rates of 30-50μs/line: it is only when the charge is read out through the amplifiers that this rate is greatly slowed down to the selected readout speed. The high cosmetic quality of OSIRIS CCD allows moving charge up and down many times before significant signal degradation occurs. In this way, it is possible to form discrete images taken at different frequencies where each area of the detector may have been shuffled into view many times to average out temporal effects in the atmosphere.

2.4 Order sorters

A Fabry-Perot Filter clearly gives a periodic series of narrow passbands. To use a FPF with a single passband, it is necessary to suppress the transmission from all the other bands that are potentially detectable. This is done by using conventional filters, called order sorters because they are used to select the required FPF order.

3. TUNABLE IMAGING VERSUS SPECTROSCOPY

For a complex instrument such as OSIRIS, with a wide variety of observing modes and submodes, one of the concerns of an applicant or a SA is whether the chosen mode is the most appropriate for the observing program to be developed. Since Tunable Imaging is a relatively new, and not widespread mode, most confusions arise between the convenience of the use of this mode versus spectroscopy.

In brief, the main advantages of TF versus spectroscopy is the ability to flux calibrate the emission (a tricky issue in MOS and even in long slit spectroscopy: slit slicing the image, differential refraction, centring errors,…), and of obtaining 2D emission line maps for targets widespread on the FOV either extended or of small size. The main disadvantage is that only one wavelength can be observed at a time. The following table and the flux diagram below help deciding the most appropriate mode.

Tunable imaging	**Spectroscopy**
1 or few spectral lines	Wide spectral range (at low R)
2D spectral features	1D (long slit) or very small area (IFU)
All targets in FOV (high ρ fields)	Number of spectra per mask limited
Reliable flux calibration	Uncertain (LS, IFU), unreliable (MOS) flux calibration
Low spectral resolution	Velocity fields & line profiles (at high R)
Approximate redshift should be known	Redshift knowledge not required
Position not required (survey) On-the-fly observations enabled. For ex: Galaxy clusters TF pre-imaging avoid IFU mosaic	Position required (pre-imaging. This introduce biases) Drilling masks overheads

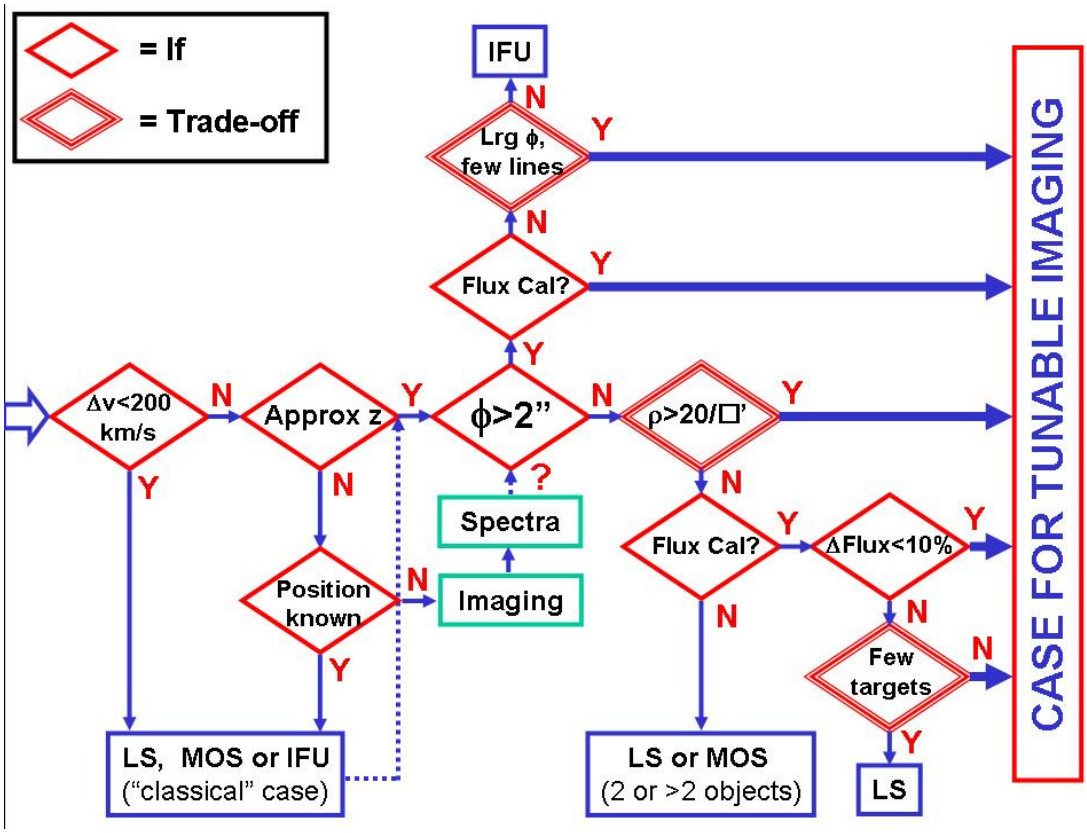

Figure 3.4.- Tree for deciding the most appropriate mode: TF versus spectroscopy. Δv is the line width or velocity dispersion, ϕ the target diameter, ρ the density of targets, and ΔFlux the error flux required.

4. OSIRIS TF CHARACTERISTICS AND FEATURES

4.1 General

The OSIRIS TF, manufactured by *IC Optical Systems*, with plate separations accurately controlled by means of capacitance micrometry, has the appearance of a conventional Fabry-Perot etalon in that it comprises two highly polished glass plates (Figure 4.1). Unlike conventional *ICOS* etalons, it also incorporates very large piezo-electric stacks (which determine the plate separation) and high performance coatings over half the optical wavelength range. The plate separation can be varied between about 3-4μm to 10 μm.

The highly polished plates are coated for optimal performance over 370–960 nm using two 'arms' (separate etalons). The coating reflectivity determines the shape and degree of order separation of the instrumental profile. This is fully specified by the coating finesse, *N*, which has a quadratic dependence on the coating reflectivity. The OSIRIS TF was coated to a finesse specification of N = 50 (red) -100 (blue) which means that the separation between periodic profiles is, respectively, fifty-one hundred times the width of the instrumental profile. At such high values, the profile is Lorentzian to a good approximation. For a given wavelength, changes in plate spacing, *d*, correspond to different orders of interference, *m*. This in turn, dictates the resolving power (*mN*) according to the finesse.

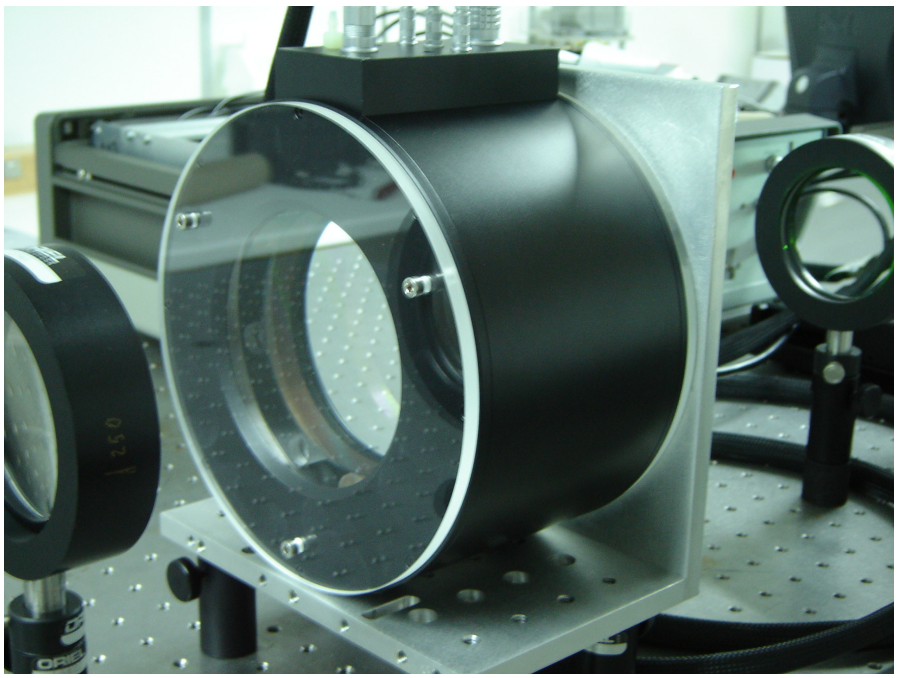

Figure 4.1.- OSIRIS red etalon at the IAC Optical Lab, while undergoing calibration tests.

In general, as can be appreciated in Eq. 2.2, for a given order, small changes in *d* change slightly the wavelength, while for a given wavelength the change of order requires a larger change in *d*. This is important to keep in mind.

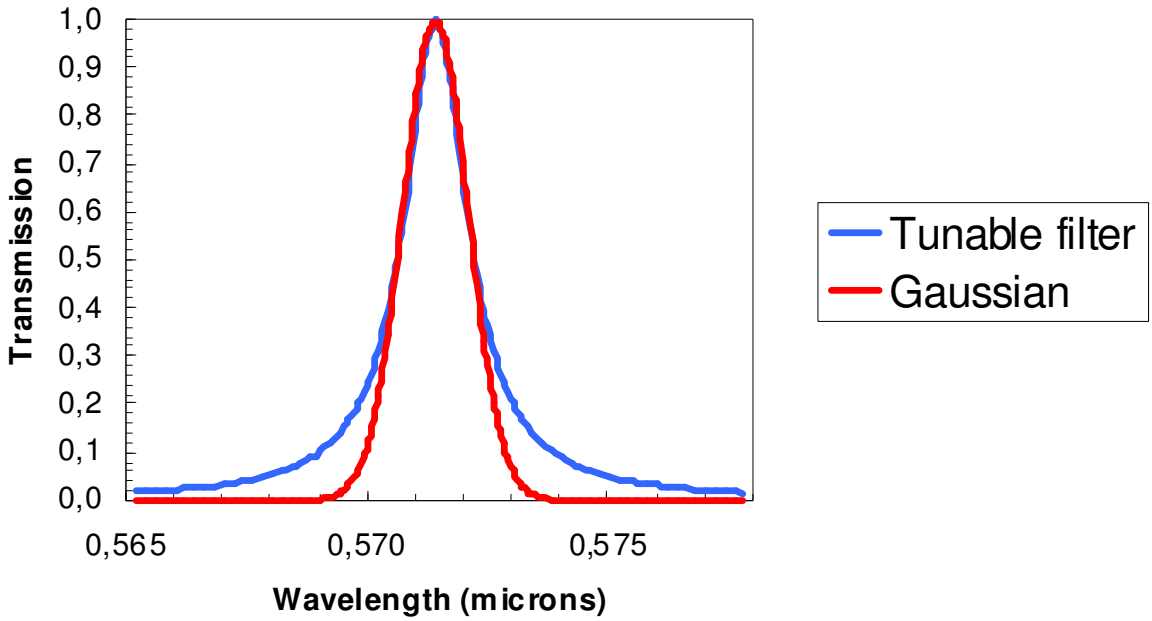

Figure 4.2.- Spectral response of a TF wrt. a Gaussian. The TF response can be considered Gaussian with a good approximation above FHWM, but is more winged below FWHM. This has to be taken into account when selecting the on and off frequencies.

With very good approximation, the spectral response of a TF, given by eq. (2.1) can be expressed by,

$$T = \left\{ 1 + \left[\frac{2(\lambda - \lambda_0)}{\delta\lambda} \right]^2 \right\}^{-1}, \qquad (4.1)$$

where λ_0 is the wavelength at maximum transmission.

4.2 Dimensions

The OSIRIS TF are model ET-100. Then the clear aperture is 100 mm diameter. The mechanical envelopes and installation procedures are provided in the maintenance manual, but OSIRIS TF are approximately 170mm diameter by 100 of thickness. Its approximate weight is of 8 kg.

4.3 Coatings

This is a critical aspect of TF performance as shown in section 2.2. For the OSIRIS TF the main difficulty is achieving a relatively constant reflectivity for a wide spectral range: from 370 to 670nm for the blue TF and from 650 through 1000nm for the red TF. This implies multilayered coatings, i.e.: thick coatings. Then the minimum distance (widest FWHM) between plates is driven by the minimum distances between the coating surfaces, not the

plate surfaces. In other words, the distance between plates (or gap) is larger. Also, since the coatings are always somewhat rugged, the coatings do not touch uniformly, but by small spots across the FOV that progressively increase their size as the plates are pressed together. Of course this is an undesirable situation since this could damage the coatings, affecting TF performance and driving to re-polish and recoat the plates, a major work that would take several months and change the performance and the calibration. However, the Inspector limits the maximum Z (minimum distance) achievable, so that in principle the TF operator can forget about this feature.

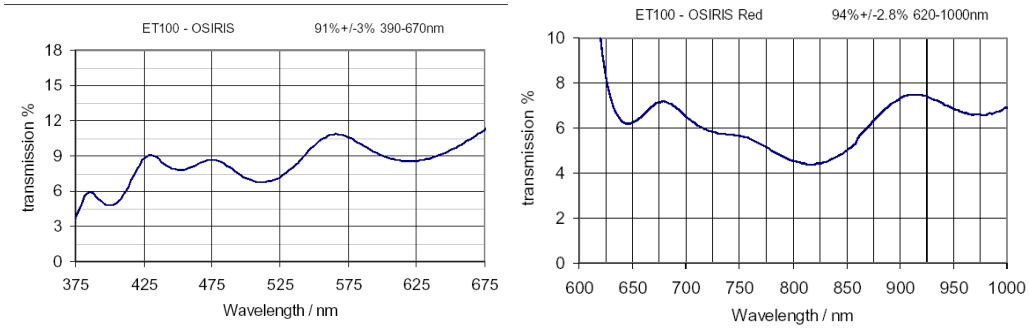

Figure 4.3.- Mean transmissions T for the blue (left) and red (right) OSIRIS TF. The mean reflectivity R = 100 – T % with a very good approximation. This results in a mean R = 91% for the blue TF and 94% for the red TF.

The wavelength dependence of the reflectivity R translates into a wavelength dependence of the FWHM range. Also, please note that the R is well behaved above 425nm for the blue TF and above 650nm for the red TF. Hence deviations are expected at lower wavelengths.

4.4 Wavelength variation across the FOV

The TF, **as any interference filter**, changes its response with the incident angle θ according to the formula,

$$\lambda_\theta = \frac{\lambda_0 \sqrt{n^2 - \sin^2 \theta}}{n} \tag{4.2}$$

where λ_0 is the central wavelength for normal incidence, λ_θ for the incident angle θ and n the refraction index.

As a consequence, and in general, it is possible to distinguish between two situations:

- Filters in a collimated beam (OSIRIS case): light beams coming from points located at increasingly distances r to the optical centre of the GTC focal plane, reach the TF at increasingly incident angles θ, with symmetry with respect to the optical centre. The incident angle on the TF (i.e.: on the pupil), is completely determined by the ratio between the telescope f_{GTC} and the instrument collimator mirror f_{Coll} focal lengths,

$$\tan\theta = \frac{f_{\mathrm{GTC}}}{f_{\mathrm{Coll}}}\tan r = 136.91\tan r\,, \tag{4.3}$$

since the **measured** focal lengths are f_{GTC} = 169888±2mm (Castro et al. 2007) and f_{Coll} = 1240.90±0.05mm (SESO 2006). The distance r to the OSIRIS TF optical centre can be obtained from the OSIRIS mean plate scale of 0.127 arcsec/pixel. Wavelength or temperature variations can be neglected, since the OSIRIS collimator is made of Zerodur, and the camera has demonstrated to be very achromatic during commissioning

Then, according to eq. 4.2 (or 2.2), there is a progressively increasing shift to the blue with respect to the central wavelength tuned (OSIRIS TF central wavelengths are tuned for normal incidence) as the distances r increase (Figure 4.4). However, since the beams coming from the same point of the FOV are parallel (the beam is collimated), the FWHM is nearly the same (Figure 4.5). This is the case of OSIRIS, since OSIRIS TFs are located in the pupil of the collimated beam. In an ideal FPF this is a pure geometric effect, and the wavelength variation is completely fixed and predictable, because it depends only on (2.2) and (4.3).

- Filters in a convergent beam (i.e.: near focal plane): beams from different points of the focal plane reach the filter with a variety of angles, that vary from point to point, but with symmetry with respect to the optical centre, and the beam is symmetric only at the optical centre. In this case, the central wavelength also shifts to the blue, but it is much more noticeable and severe the FWHM increase and the corresponding transmission reduction (Figure 4.5). Also, an etalon must never be placed into the focal plane, since coating heterogeneities are then "seen" instead of averaged by the collimated beam, and a varying spectral response as a function of target position is produced.

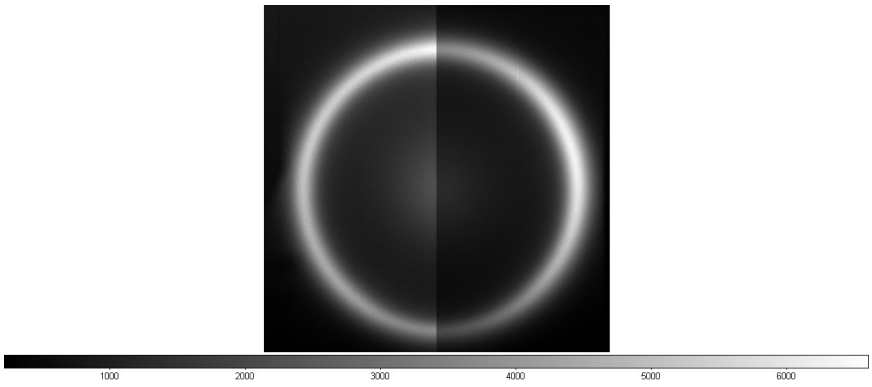

Figure 4.4.- Image of a Ne spectral lamp uniformly illuminating the TF tuned to a central wavelength to the red of the observed Ne line. A ring forms due to the central wavelength variation across the OSIRIS FOV. Both CCD detectors are shown without including the gap.

However, as already stated in Section 2.2.1, equation (2.2) apply to ideal FPFs. Really, the full expression of equation (2.2) is:

$$m\lambda = 2\mu\, d\cos\theta + 2\mu_c d_c \cos\theta\,, \tag{4.4}$$

where μ_c and d_c are the effective refractive index, and the coating thickness of the reflective coating, respectively.

This additional term in (4.4) can be neglected when $d >> d_c$, as is the case for high resolution FPs, since d is of the order of hundreds of microns, while d_c is of the order of microns, but not in FPF, where both are of the same order of magnitude. The contribution is more severe when the coatings are thick, in other words, when the wavelength range covered is wide, as is the case of most FPF, and certainly of OSIRIS TFs. Also, the additional term depends on wavelength, since both refractive index and coating thickness depend on wavelength, and this dependence is non-linear. The effect can be noticed even for normal incidence ($\theta = 0$), producing effective etalon gaps that are wider than expected, and hence FWHMs that are narrower than expected, and that depend on wavelength. This has been observed mainly in the OSIRIS blue TF, specially between ~490 and ~590nm. The FWHMs can, however, be considered nearly constant within the whole OSIRIS TF FOV.

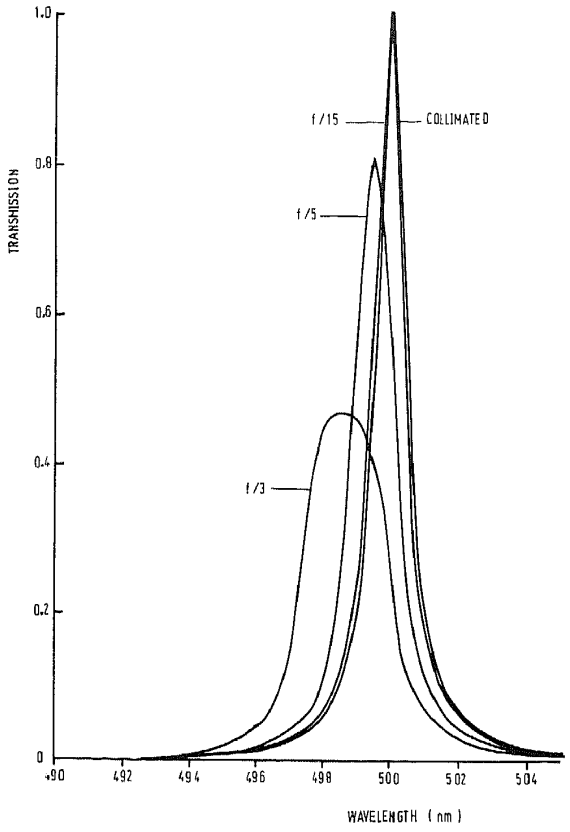

Figure 4.5.- Change of FWHM and transmission of a filter into a convergent beam. The faster the beam, the more severe the effect. From Atherton et al. 1981.

For this reason, the wavelength variation of a FPF across the FOV does not follow a pure geometrical dependence as that given by the combination of (2.2) and (4.3). This effect was first reported by Veilleux et al. (2010) for the TF of the Magellan-Baade 6.5m telescope.

These authors detected variations of the wavelength dependence across the FOV, that depended non linearly on etalon gap and wavelength, and that they attributed to variations of the focal distance of the camera, although clearly this cannot be the origin of this effect (González et al. 2012).

For calibrating the wavelength dependence across the FOV for the OSIRIS red TF, images of different emission lines at different wavelengths, covering the full OSIRIS wavelength range, were obtained (courtesy of A. Cabrera-Lavers). For each emission line, the red TF was tuned at different wavelengths. The results were checked against OSIRIS TF data of cluster galaxies covering the whole OSIRIS FOV, courtesy of M. Sánchez-Portal, with spectroscopy available from the literature. From these data, the following wavelength dependence across the OSIRIS FOV **for the red tunable filter** is derived,

$$\lambda = \lambda_0 - 5.04 r^2 \tag{4.5}$$

where λ_0 is the central wavelength tuned, and r is the distance in arcminutes to the optical centre of the TF, that is located at (−11±1, 976±1) pixels with respect to CCD2. Equation 4.5 implies that the wavelength dependence is lower than expected, and independent of wavelength as a first approximation (but see below).

Within the inner ~2 arcmin, this expression is very accurate for any wavelength (Figure 4.6). Even at the edge of the 8 arcmin diameter OSIRIS TF FOV, the maximum error is of the order of the tuning accuracy (~1-2Å) for most wavelengths, and always within ±6Å in the worse cases (Figure 4.6). This accuracy is enough for most applications, given the TF tuning accuracy already mentioned, and that if images are dithered, an additional wavelength shift depending on the distance to the optical centre is produced. For example, at the edge of the 8 arcmin diameter TF FOV, the shift is of ~7Å for a dithering of 10 arcsec.

For those specific projects requiring more accuracy, that use no dithering, an additional chromatic term $a_3(\lambda)$,

$$\lambda = \lambda_0 - 5.04 r^2 + a_3(\lambda) r^3 , \tag{4.6}$$

with $a_3 = 6.1781 - 1.6024 \cdot 10^{-3} \lambda + 1.0215 \cdot 10^{-7} \lambda^2$, where λ is in Å, allows obtaining accuracies of the order of the tuning error (±1Å) within the whole OSIRIS TF FOV.

In the above expressions the distances r are not corrected for distortion (i.e.: are before applying astrometric corrections).

The corresponding expressions for the OSIRIS blue TF will be derived as soon as it is commissioned.

For more details about the calibration procedure, the dependencies analyzed with respect to mode, rotator angle and temperature, and the formal derivation of the analytic expressions from (2.2), see González et al. (2012).

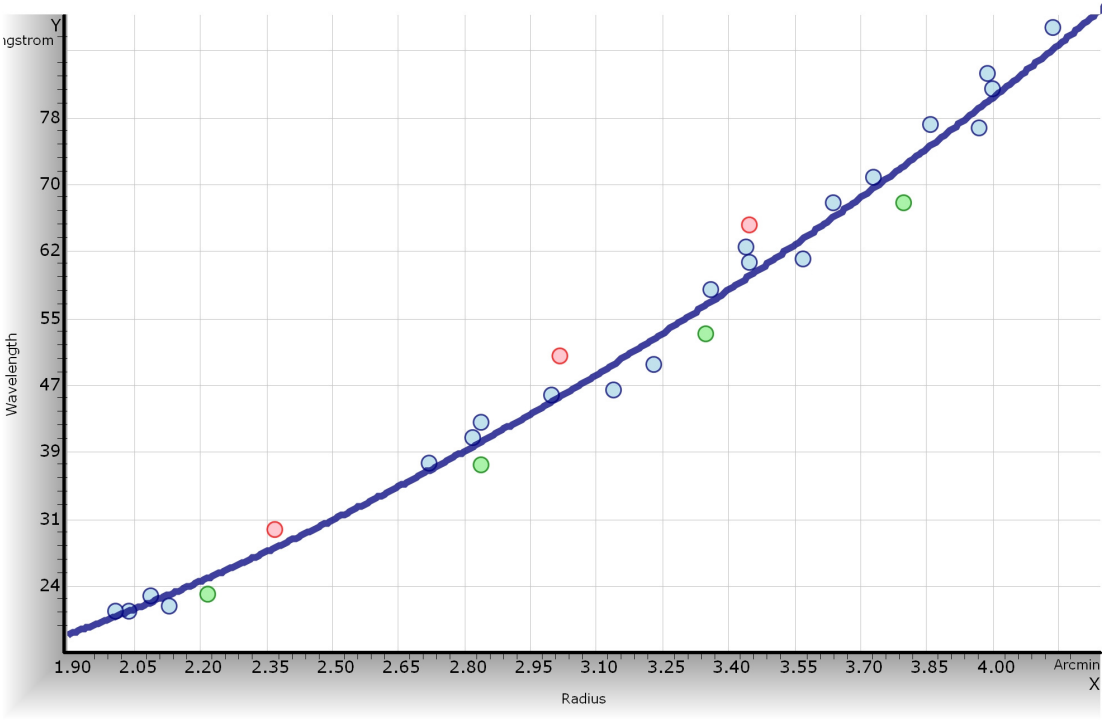

Figure 4.6.- (λ_0-λ) vs. radius for different emission lines from the ICM spectra lamps covering the whole OSIRIS red TF wavelength range. The curve is the equation (4.5). In red and green are the points that depart most from (4.5), corresponding to Hg(Ar) 7635Å and Xe 9162Å, respectively.

4.5 Ghosts

One feature of etalons is that they produce ghosts. In any astronomical instrument, the detector is a source of light: any light that is not detected or absorbed is reflected. This light reflected by the detector follows the same optical path in opposite direction (according to the principle of reversal light in an optical system), entering the etalon and reflecting in the most reflective surface, i.e.: that of the reflective coating of the etalon cavity, going back and hitting the detector in a place symmetric with respect to the optical centre of the etalon. This has two important implications for the observer

1. Diametric ghosts are symmetric with respect to the centre of the etalon (Figure 4.7), that in the case of OSIRIS is almost the centre of the OSIRIS field: in the gap between detectors at the line ~1990. But not the centre of the telescope field since OSIRIS is off axis, and then is not the pointing centre.

2. Diametric ghosts can be easily removed by the classical dithering procedure since moving the image in one direction shifts its ghost in the opposite direction with respect to the TF optical centre. Then when piling up the images taking as reference the image of the target, all ghosts fall in different pixels and can be removed with average sigma clipping of similar algorithms

3. Only very bright, usually saturated sources, generate ghosts (Figure 4.7). Hence, unless very bright sources are in the FOV and their ghosts could spoil the image of the target, there are no need to worry

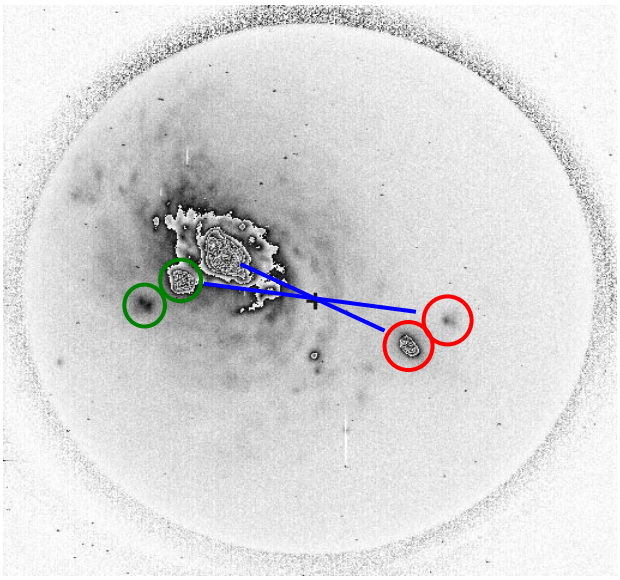

Figure 4.7.- Example of ghosts in a tunable filter. The cross marks the optical centre. The red circles mark the diametric ghosts of the centre of the galaxy and that of an exponential ghost, while the green ones marks the exponential ghosts. The second exponential ghost does not produce a noticeable diametric ghost.

Of course ghosts drives the location of the target in the FOV, as is dealt with further on in this document in Section 5.

Exponential ghosts cannot be removed by dithering. Luckily OSIRIS TF does not have this kind of ghosts.

4.6 Calibrations required

In general, as described in 2.2.3, three piezos control the separation between the plates. An exact control of the piezos is achieved via the etalon controller CS-100 of ICOS. However, for the purpose of a user manual, the TFs are controlled via the Inspector interface (that send specific commands to the CS-100 though). Then the user can forget about operating the CS-100 directly, although sometimes some comments are included for the sake of completeness.

4.6.1 Paralellism calibration

The piezo expansion or contraction is achieved by varying the HV supplied. The plate separation is non-linearly and differentially measured by capacitance bridges in terms of bits

(Figure 2.3). Each bridge provide, then, the relative separation with respect to two perpendicular axes, whose value in bits are termed X and Y.

Then, regulating X and Y is necessary for achieving plate parallelism. The price to pay for a slight lack of parallelism is a reduction of the peak transmission, and an asymmetry of the spectral response.

Due to the thick coatings of OSIRIS etalons, the parallelism depend both on wavelength and the order. This is a weak dependence for the red etalon but more noticeable in the blue. The CS-100 has been programmed to compensate for this variation in the blue etalon[1]. However, the **parallelism values are very stable in time and no changes has been detected so far** (worth periodically checking anyway).

4.6.2 Wavelength calibration

Once the etalon is parallelized, then all piezos act co-ordinately (keeping parallelism while increasing or decreasing plate separation in closed-loop operation of the CS-100), and the plate separation is non-linearly quantified in bits by means of the parameter Z (in bits).

Essentially, **wavelength calibrating an etalon means establishing the dependence between wavelength and Z for the different orders** (i.e.: FWHM). This dependence is a function of wavelength and order. For this reason, the calibration should be performed near the wavelength and order of interest.

Wavelength calibration depends, at least, of the following:

- Day to day variation. For this reason it is advisable calibrating before every observing run. This dependence is barely noticeable in OSIRIS since is masked by temperature variations

- Humidity. This is likely the most severe, although it can be ignored in OSIRIS since the instrument is flushed with dry air[2]

- Temperature. This is a highly non-linear effect where the etalon undergoes several phases of different variations. ET100 are quite large and take up to three hours to stabilize versus temperature changes. However this is not as serious as it seems, since implies only calibrating more frequently, depending on the history and the temperature gradient. It has been demonstrated to be safe operating with TF temperature gradients of at least 0.6ºC/hour, produced by temperature differences between TF and telescope of several degrees, as long as calibration is checked every 20 or 30 minutes. When the temperature gradient is of the order of 0.1-0.2 ºC/hour the tuning can be considered stable for at least one hour. However, in a future version of the instrument control, the Inspector will take care of this effect at user's request

[1] Please confirm this implementation with OSIRIS responsibles.

[2] However, caution must be taken when opening the instrument for changing filters or masks shortly before observations. See environmental conditions in user manual.

- TF position. Depending on instrument rotator angle. Up to now extensive and painful tests have been done during several nights at different wavelengths and orders. The results are not conclusive: sometimes the tuning changes others not, without any apparent relation with wavelength, order, temperature or whatsoever. However, a range of rotator values where this wavelength variation, if present, is more severe, has been identified: **from –30º to +60º**. It is advisable avoiding it whenever possible. Otherwise, calibrating to compensate TF temperature variations should be enough to compensate for that effect as well. The possible origin of this variation with orientation could be attributed, for example, to relative mechanical shift of the plates of the reference capacitor that thus change its capacity.

- TF history: if plates collide, the TF calibration might change. This is unlikely to happen since the Z range has been limited to safe values. However, caution must be taken when reaching values around or above Z = 40000 (for the red, for the blue is still TBD)

There are several ways for parallelizing and wavelength calibrating a TF. The practical procedure used for OSIRIS is described in section 7.

As a rule of thumbs, when Z increases (gap decreases) a little bit (by hundredths), the central wavelength shifts to the blue, i.e.: when observing a ring (Figure 4.3), the ring shrinks. When Z varies several thousandths, i.e.: a FSR, the mode changes (and the wavelength as well). The larger the Z (smaller the gap), the larger is the FWHM.

4.7 Tuning accuracy

The theoretical tuning accuracy is 0.02 nm in wavelength and FWHM as provided by the CS-100 etalon controller (in most cases this is the typical value of 1 bit in Z). The real accuracy is driven by the wavelength calibration accuracy, that can be of the order of 0.1-0.2nm.

4.8 Tuning speed

The tuning can be changed in an interval between 10 to 100ms, depending on the change in Z. Really, for large Z differences, the TF control system automatically move the etalon in steps to avoid “out of range” failures. For fast modes it is advisable limiting the range of Z movement to the minimum (hundreds).

4.9 Tuning range

The tuning range is driven, at the smallest plate separations (lowest resolution, largest TF FWHM), by the coatings touching, while at the largest separation (higher resolution, smaller TF FWHM) is driven by the order sorter filters, that are designed to block orders at a certain TF FWHM, since the different orders become closer as *m* increases (FWHM reduces). The OS filters are designed to block orders for a minimum FWHM that is of 1.2nm for the red TF and between 0.6 and 1.2nm (TBC) for the blue TF. Then, although the plates can be separated more than specified, i.e.: the FWHM reduced below 1.2nm, the OS do not guarantee that other orders do not enter the nominal field of 8 arcminute in diameter. Narrower OS FWHM would be required for using TF FWHM below 1.2nm (for the red TF). However, depending on the position of the central wavelength with respect to the OS

operating wavelength range, the FWHM could be reduced down to 0.6nm (for a wavelength centred with respect to the order sorter operating wavelength range). This "trick" must be used with caution and only by experienced (and warned) observers.

4.10 OSIRIS TF FOV

According to the above, **the OS guarantees a FOV free or other orders of 8 arcminutes in diameter**.

Although OSIRIS TF were originally specified for minimum FWHM of 1.2nm over the whole wavelength range, the blue TF coatings are thicker, and then the minimum plate separations are larger, resulting in a minimum FWHM that is not driven by the order sorter, as in the red. On the contrary, the OS have been chosen according to the maximum FWHM attainable with the blue TF.

Order sorters overlap in wavelength and their wavelength range where is guaranteed that they suppress other orders is smaller than their FWHM (Appendix B). This is because OS are tilted 10.5 degrees with respect to TF and grisms, to avoid ghosts due to backwards reflections from the detector (the TF is not tilted and then have these reflections as explained above). The tilting axis is, with enough approximation, the detector gap.

5. OBSERVING STRATEGIES

The observing strategies for a TF are driven by the following instrumental effects:

1. The spectral response of the TF: more peaked and with more wings than a Gaussian or a squared 5-layer interference filter (Figure 4.2).

2. The diametric ghosts

3. The centre to edge wavelength variation

and affects the way to design an observation depending on the characteristics of the sources:

- Photometric accuracy requested. **Please note that from now on we will refer to photometric accuracy of instrumental origin, not due to readout or photon noise**.

- Possible neighbouring lines to the one studied

- Velocity field or line width of the target

- Size of the target

- Redshift of the target

playing with the possible variables:

- TF central wavelength for your On and Off images

- TF FWHM
- Position of the source in the FOV
- Rotator position

These mark the difference with respect to direct imaging with conventional filters, and of obtaining useful data instead of wasting observing time obtaining useless data. In other words, in tunable imaging the design of an observation is extremely important, as the observing procedure is.

In the following sections will derive recommended observing strategies depending on the type of sources, and the scientific aims, by playing with the previous parameters.

5.1 Selecting off band

5.1.1 Continuum subtraction

In line imaging, two images are usually required: the on-line image and the off-line (or continuum) image. The on-line has line plus continuum photons and the off-line only continuum photons, to be subtracted from the on-line image to give the emission line (continuum free) image.

This can be done in two ways:

1. Using the TF for line and continuum has the advantage that the spectral response and FWHM is the same, and that you can select the continuum as near as desired from your line, thus alleviating possible continuum variations with wavelength. It is even possible, using the technique of shuffled exposures (Section 8.3) to on-line averaging continuum on both sides (blue and red) of the line and averaging possible seeing and atmospheric variation. Then it is possible to achieve a very good continuum and sky subtraction with a direct pixel-to-pixel difference between your on-line and your continuum image. However, TF have quite narrow FWHM and the exposure times are quite large.

2. Using a medium band (and OS) or broad band filter (SDSS). In this case continuum subtraction is not as good, and certainly not as direct, and must be faced with caution. This document is not intended to be a manual for continuum subtraction, there are many different techniques that can be used, that will not be dealt with here. However, since now the continuum filter is tens of times wider that TF, the exposure times required are reduced accordingly.

5.1.2 Off-band wavelength and FWHM tuning selection

If the TF is to be used for continuum subtraction, the TF tuning of the off-band has to be chosen so that no or few emission enters into the continuum filter. This is driven by the photometric accuracy required via the following expression, derived from Eq. (4.1),

$$\frac{|\lambda-\lambda_0|}{\delta\lambda}=\frac{1}{2}\sqrt{\frac{1-T}{T}} \tag{5.1}$$

This equation can be interpreted, in this case, as providing the transmission *T*, normalized to unity, of your continuum filter, tuned at λ_0 and of FWHM $\delta\lambda$, at the wavelength λ of the on-line tuning.

For example, let assume that the continuum must be chosen with a contribution from the emission line lower that 5%. Then, for a given FWHM of say 1.8nm, the tuning of the continuum must be placed 4nm away from the line tuning. Of course wider FWHM require increasing the wavelength difference between on and off-line tunings.

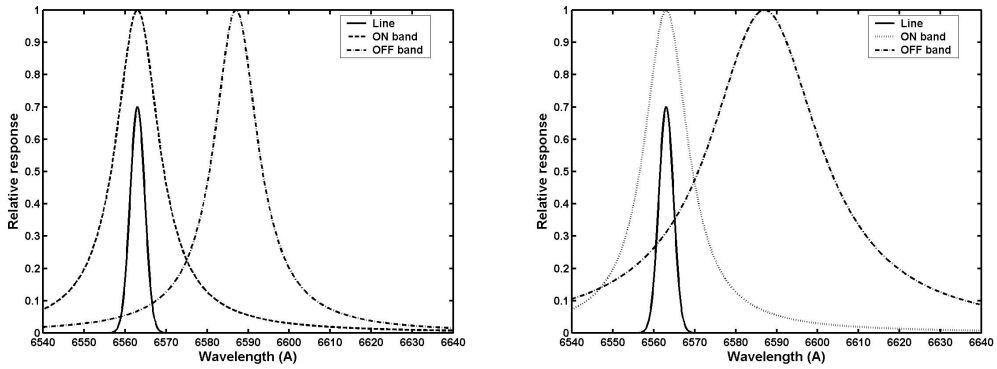

Figure 5.1.- Left: A proper tuning of the off-line wavelength minimizes contribution from your line to the continuum according to Eq. (5.1). Right: Increasing the FWHM of the off-line tuning will require increasing the wavelength difference between on and off-line wavelength tunings. The distances are larger than expected since the TF spectral response has more wings than a standard interference filter.

5.2 Deblending lines

Equation 5.1 can also be used for deblending lines. Known the redshift, one tuning for each line can be observed. From the line separation and the FWHMs of the tunings, the contribution of the other lines to each tuning can be estimated, and corrected simply via simultaneous equations system.

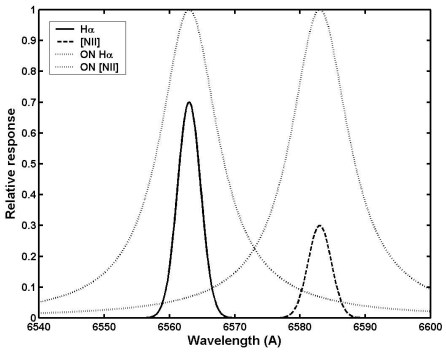

Figure 5.2.- Hα can be deblended from [NII]658.4nm if the redshift or Doppler shift is known, via defining a simultaneous equation system with TF transmissions derived from the TF FWHM and line relative positions.

5.3 On-line FWHM selection

The TF FWHMs are quite narrow, and nearly Gaussian from peak to half transmission. Then the line width must be quite narrower than the TF FWHM or otherwise some flux will be lost. It can be easily demonstrated that, assuming Gaussian line profiles, the flux error can be approximated by,

$$\text{Flux error}(\%) = \frac{1}{2\ln 2}\left(\frac{\delta l}{\delta \lambda}\right)^2 \tag{5.2}$$

where $\delta\lambda$ is the TF FWHM and δl is the line width. For example, observing a line with the same width than the TF will drive to loosing ~28% of the flux (a more precise calculation gives 36%).

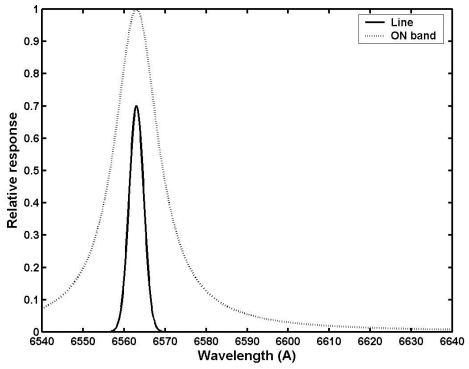

Figure 5.3.- Comparison of TF and line profiles.

The following table can be used for selecting to most suitable FWHM according to the expected line width. Please note that they are approximate values.

$\delta\lambda/\delta l$	**Flux error (%)**
1.0	36
1.5	22
2.0	14
2.5	10
3.0	7
3.5	5
4.0	4

Table 5.1.- Approximate error fluxes depending on line width (δl) and TF FWHM ($\delta\lambda$).

For example, the typical velocity field of a spiral galaxy (250 km/s) at zero redshift, would require TF FWHM of at least 1nm at Hα, for an error smaller than 5%[3], and the minimum FWHM recommended for the red TF is of 1.2nm. Hence this is not a problem in this case, but it might be for [OII]372.7nm (blue TF) or when observing objects at significant redshifts where the line widths are expanded[4] by the factor (1+z). Since the range of available FWHM are quite limited, if a certain photometric accuracy is required and the needed FWHM cannot be obtained, it is possible to synthesize a wider FWHM by summing images of a scan (see further on in this document).

5.4 Deciding target position and orientation

The presence of ghosts and the centre to edge wavelength variation drive target position on the OSIRIS FOV.

To avoid excessive wavelength variation, the target should be as centred as possible, but it cannot be placed in the centre because, aside of falling into the gap between detectors, a mirrored ghost image of the source will overlap with the real image. This might be acceptable in some cases, for example if the user is interested in radial dependences only. However, in general, the target should be placed near the optical centre of the TF, but fully off it. Near the TF centre but on CCD2 (the rightmost) is a convenient place.

If the object is elongated, the wavelength variation can be minimized by turning the GTC rotator to align the major axis of the target perpendicular to the radial direction for the TF optical centre (Figure 5.4).

However, since the target is not at the centre of the TF, the TF must be tuned to the red of the line, so that the target is observed at the wavelength of the line required. This can be evaluated using Eq. 4.3. For example, a target of a diameter of 2 arcminutes should be placed somewhat more than 1 arcminute from the centre. Then the wavelength corresponding to the zero redshift Hα at this position is not 656.3nm but 656.8nm.

Even with the above strategy, and unless the target is very small, the wavelength dependence across the FOV will produce that some parts of the target are observed at different wavelengths. The induced photometric error can be evaluated using Eq. 4.3 and 5.1. For example, for the same example above, the wavelength of the edge of the target near the TF centre is 656.8nm and the wavelength at the edge of the target in opposite direction is 654.7nm. The photometric errors induced by this line decentring are, respectively, 7% and 45% (from Eq. 5.1) if a FWHM of 3.5nm is assumed. Then, it is possible to choose a TF tuning wavelength that minimizes this variation: when the wavelength difference at both edges of the target is the same. For example, tuning at 657.3nm gives a photometric error equal at both edges of the target and of the order of 25%. Of course **the velocity field of the target must be taken into account in this procedure** since it increase the photometric errors (if the velocity field is known, it is possible to play around with the target and rotator position to minimize it).

---

[3] Please note that 250km/s is the FULL velocity field, not the velocity field at FWHM.

[4] Please do not forget this “detail”.

Were this photometric error too much, it is possible to synthesize a wider FWHM by adding TF scans (see 5.7).

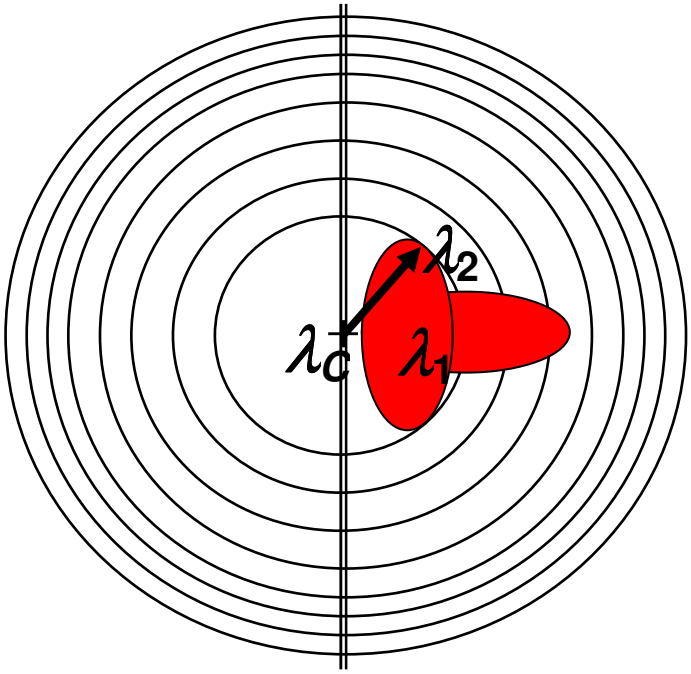

Figure 5.4.- Changing rotator angle is useful for minimizing the wavelength variation across the target.

5.5 Removing ghosts, cosmic rays and cosmetics

As stated above, ghosts can be removed using the same dithering that remove cosmic rays and detector cosmetics. However dithering move targets on the TF FOV, i.e.: changes the wavelength at which the target is observed. This is specially severe at the edges of the FOV, where the wavelength variation is larger (Figure 4.5). There are several ways to alleviate this problem that will be described in the following subsections. Anyway, please note that in many cases ghosts do not required to be removed, since they can be seen only for very bright sources, and are diametric so that they can be readily identified.

5.5.1 Half field masking

Inserting a half-field mask that hides detector CCD1 avoids ghosts coming from that part of the field. Then no dithering is done and cosmic rays can be removed by specific programs since the pixel size is small enough (0.127 arcsec) so that a cosmic ray cannot be confused with an astronomical target even in good seeing conditions (binning and seeing depending, of course).

However, in this case only half the field can be used, then this is not the optimal technique for observing blank fields.

5.5.2 Azimuthal dithering pattern

When only one relatively small source is of interest, the dithering can be done following the circle of equal wavelength.

5.5.3 TF tuning dithering pattern

If several relatively small targets spread on the FOV are to be observed, it is possible to do a three point dithering where the TF tuning is changed to minimize wavelength variations at the edge of the TF FOV in **one direction**. Then different sections of different images can be combined. This is valid only when using tunable tomography.

5.6 Tunable tomography

5.6.1 Technique

Tunable tomography or TF scanning consist in obtaining a set of images of the same pointing at different consecutive wavelengths (Figure 5.5). The characteristic parameters are:

- Initial and final wavelength (or Z)
- Step in wavelength $\Delta\lambda$ (not equivalent to a constant ΔZ since the λ–Z relation is in general not exactly linear)[5]

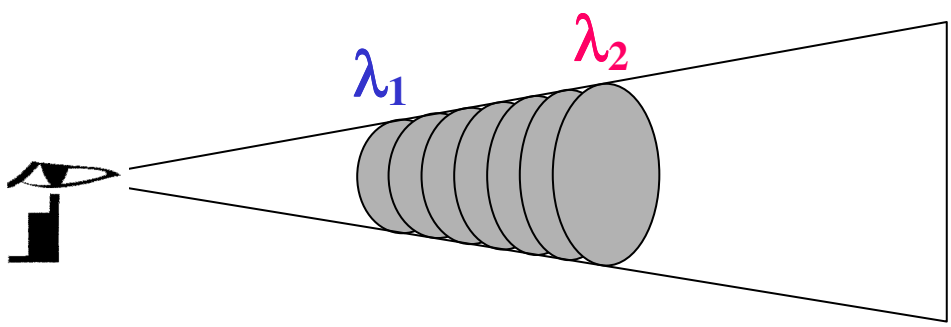

Figure 5.5.- Tunable tomography consists in scanning a wavelength range using the TF. For the same telescope pointing, a set of images at different wavelengths are taken.

The step must be carefully chosen since for a given wavelength range to be scanned, a step too fine will increase the observing time and overheads required, but a step too coarse would introduce larger photometric errors, that can be evaluated using Eq. 5.1, but now considering that the maximum error will be half the scan step (i.e.: in the worst situation an emission line would be located in the middle of a step),

$$\frac{\Delta\lambda}{\delta\lambda} = \sqrt{\frac{1-T}{T}} \,. \qquad (5.3)$$

[5] Please note that further on this document $\Delta\lambda$ is NOT the FSR of Eq. 2.5 and 2.7, but the scan step or wavelength step between consecutive exposures in tunable tomography.

In this observing mode, the different images are not combined, but analyzed separately. Usually aperture photometry of the sources of each image provide "pseudo-spectra" that are used for identifying emission lines and determining its fluxes and Doppler shifts or redshifts.

In the case that the TF images are going to be used for continuum subtraction, the images of the same scan (or several of them added together) can be used for this purpose, as long as they are separated enough to achieve the required photometric accuracy based on TF FWHM, scan step and the number of images (Sec. 5.1.2). This might require obtaining some additional images at the end and/or the beginning of the scan (at the end and beginning would allow averaging possible continuum variations).

5.6.2 Some applications

- Scanning a spectral region for deblending neighbouring lines
- Scanning a target looking for systems of high velocity faint or diffuse ionized gas
- Scanning blank fields searching for serendipitous emission line targets (for example: OTELO and HORUS surveys) in a certain volume of universe determined by the FOV and the initial and final wavelength for every emission line detected
- Scanning the velocity field of galaxy clusters allows determining emission line objects and even the cluster velocity dispersion (for example: GLACE survey)
- Scanning a certain emission line of a target of inaccurate redshift

5.7 Band synthesis technique

5.7.1 Technique

As before, but in this case the final destination is not analyzing images separately but adding them together providing a "wider" synthetic filter (Figure 5.6).

The main difference is that in this case one additional image must be obtained at the beginning and at the end of the scan (in a conventional filter equivalence this would be similar to the zone where the spectral response is varying and the flat zone has not been reached yet), and that the photometric accuracy refers to the wiggles generated when adding the images (Figure 5.6). Alternatively instead of obtaining this "extra" images, it is possible to correct them by multiplying by the appropriate factor > 1 that can be easily calculated.

As a guideline, the photometric accuracy that can be achieved as a function of the scan step is summarized in the table below (Figure 5.6).

$\Delta\lambda/\delta\lambda$	$\delta I/I$ (%)
1	20
2/3	5
1/2	2

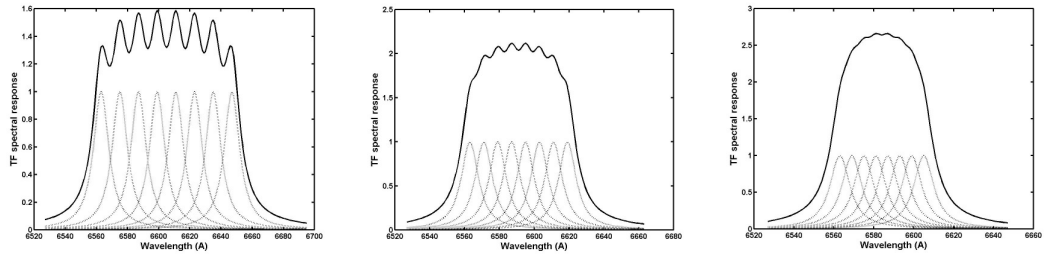

Figure 5.6.- Theoretical examples of the band synthesis technique. Left: a scan step equal to the TF FWHM gives photometric uncertainties of ~20%. Middle: a scan step 2/3 of the TF FWHM gives photometric uncertainties of ~5%. Right: a scan step equal to half the TF FWHM gives photometric uncertainties of ~2%. The first and last images are either not used or corrected via the corresponding multiplicative factor.

Of course the images obtained can be used both for Tunable tomography and band synthesis. For example: in tunable tomography, images can be combined in, for example, pairs or terns to increase S/N in the case of faint targets (depending on line widths and TF FWHM), or all added together to serve as pseudo-broad band image for target detection.

5.7.2 Some applications

- Scanning the velocity curve of a large spiral galaxy compensating for the centre to edge wavelength variation

- Scanning a wide spectral line (i.e.: that of a high redshift galaxy or a QSO)

5.8 Sources of instrumental photometric errors. Summary

Then the sources of photometric errors of instrumental origin (again, please note that contributions of readout or photon noises must be considered aside) are:

- The FWHM of the TF, depending on line width (driven by velocity dispersion, velocity field, peculiar velocities, and redshift). Can be evaluated using Eq. 5.2 or Table 5.1. If required can be corrected using the method of band synthesis (Sec. 5.7).

- The contribution of the line to the off-band or to other lines to the on-line image. Can be evaluated using Eq. 5.1

- The wavelength variation across the target. Depends on the size and the velocity field. Can be evaluated using Eqs. 4.3 and 5.1. If required can be corrected using the method of band synthesis (Sec. 5.7).

- Dithering that varies the wavelength of pixels of the source from one image to a dithered one. Can be evaluated using Eqs. 4.3 and 5.1. If required can be corrected using the method of band synthesis (Sec. 5.7) or choosing a suitable dithering pattern combined with TF tuning (Sec. 5.5.2 and 5.5.3).

6. STARTING UP OSIRIS TF

- On the CCCS (see CookBook) power on the TF, were it not powered on before

- On the TF menu of the OSIRIS Inspector, click on "Init". XYZ should be set to some reasonable default values after few seconds and the OSIRIS/MCS/TFComp info pass from "ON" to "IDLE" status (Figure 6.1)

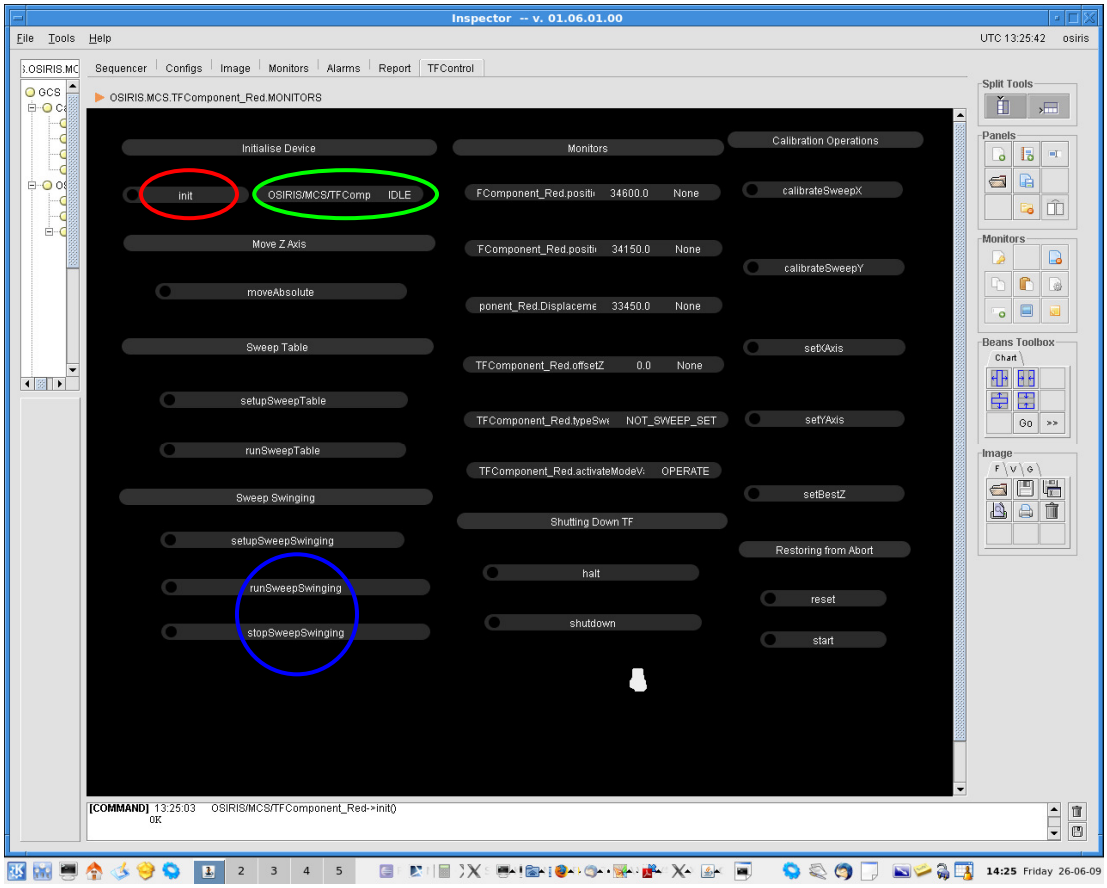

Figure 6.1.- TF panel of OSIRIS Inspector. Init banner is located at the top, left, below "Initialize Device",marked with a red circle. The system is in "IDLE" state (green circle): ready to operate with HV activated.

- Now ("IDLE" status) the high voltage is applied to the TF piezos and **the instrument must not be powered off till the TF have been properly shut down** (see Sec. 11)

7. CALIBRATING OSIRIS TF

7.1 Parallelism

7.1.1 General considerations

As mentioned above, TF parallelization consist in determining the X and Y values that keep plates parallel, and depends on Z and λ. OSIRIS TF Parallelism is **very** robust, and do not vary with time even when switching off and on again the TF controller. Hence, once the XY values for a certain Z and λ range are determined, they can be used around these Z and λ values from then on. Checking parallelism values from time to time are recommendable though.

Then, it is strongly recommended that SAs keep track of the XY values obtained versus Z and λ, noting down rotator position and TF temperature gradient on a daily basis. A summary table of these values should be updated accordingly and made readily available in the control room for daily operation.

The parallelism variation changes are more noticeable near high Z values and at the reddest λ. In general, XY should be checked in ranges of, say, 5000 in Z and 50nm in wavelength (more frequently beyond 850nm, were coatings vary most).

A table with the parallelism values determined so far is included in Appendix C.1.

7.1.2 OSIRIS TF parallelization procedure

The easiest way to parallelize an etalon is visually observing the rings obtained using viz. a fluorescent light and hand tuning XY using the CS-100. Since the parallelism is very robust, it will be kept after switching off the CS-100, and mounting the TF on the instrument. However, a procedure for parallelization with the TF mounted in the instrument is necessary, specially bearing in mind that there is a parallelism variation with Z and λ. Several procedures have been devised to this purpose and here a suitable one is described both for parallelism and wavelength calibration.

This parallelisation procedure for the TF is a task to be done during Day time.

The basis consist in maximizing the intensity of the light in the optical centre of the TF, when tuned for observing an emission line coming from a calibration lamp, when varying X and Y. This is the same procedure to be employed for wavelength calibration, but then varying Z. A lack of parallelism (XY) or a lack or tuning (Z) will reduce the intensity measured. This procedure is achieved by inserting a wide centred long slit, and charge shuffling the charge on the CCD while varying X, Y or Z from shuffle to shuffle.

From now on, N will be the number of steps in X, Y or Z. ΔX, ΔY and ΔZ the X, Y or Z increments in bits, respectively, from one step to the following, Xi, Yi and Zi the initial X, Y or Z values, respectively, and n the step (counting from the first one) were the line is brightest.

This procedure has, however, some very important points to keep in mind:

- The light must be stable. Then several minutes should pass after switching lamp on, and exposure times larger than 100ms must be used to get rid off AC electric power variations and shutter accuracy

- **Single**, intense emission lines must be used. No other line (unless very weak) must be in about 10nm both sides of the spectra

- The TF must be tuned to the line (i.e.: the Z must be the one corresponding to the emission line)

The last requirement implies an iterative procedure to calibrate XY and Z sequentially. In detail is as follows:

1. Switch the selected lamp on (first thing to do to allow it warming up and reducing calibration time) and the dome lights off

2. Set rotator at the requested value for observations (try avoiding the range −30º to +60º)

3. Insert the calibration mirror

4. Insert the long slit of 2.5 arcminutes (this is a special one for this type of calibrations, any other could be used instead, as long as it is not narrower).

5. Using the tables of appendix B, and/or the TF calculator, set approximate XY values for a given line of Z and λ nearby the ones required

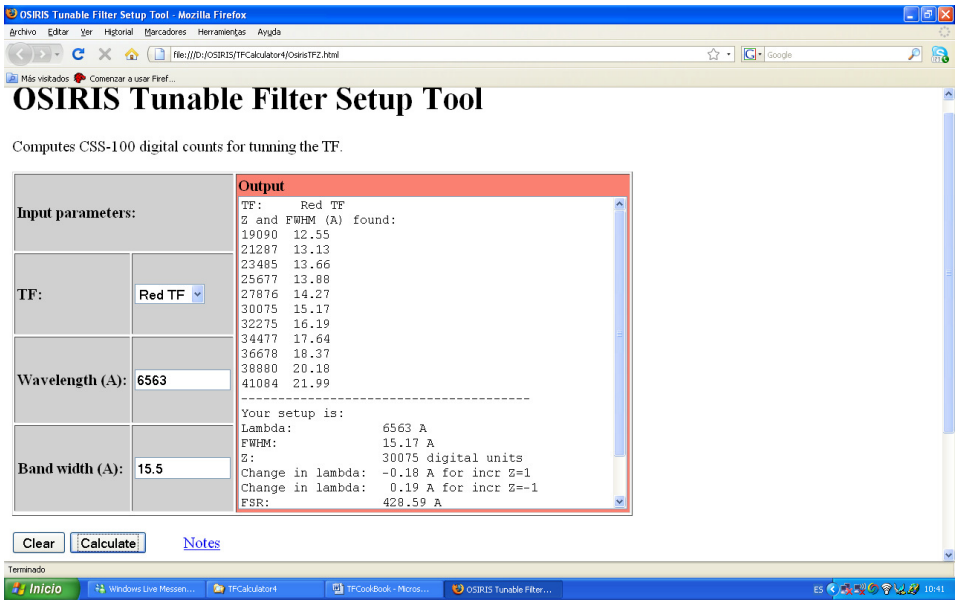

Figure 7.1.- Basic TF Calculator. Given the TF, wavelength and bandwidth, returns Z, nearest FWHM, and the slopes λ/Z to the blue (ΔZ=+1) and to the red (ΔZ= −1) of the predicted Z. FSR is provided as well, for etalon lovers. Java-XML script courtesy of J.I. González-Serrano based on Guillermo Herrera filtered data obtained at 10.5ºC. See TF calculator notes.

6. Take a set of exposures charge shuffling the CCD and varying Z from exposure to exposure ±100 bits of the value predicted by the TF calculator. It is advisable using 20 steps of 10 bit each. In other words: N = 20, ΔZ = 10, Zi = Z predicted – 100. This resolution is equivalent to, approximately, 0.2nm and it is possible to calibrate to half this, i.e.: 0.1nm, that is the goal to be achieved. Alternatively, the first time ΔZ = 10 can be set, and afterwards ΔZ = 5 can be used. However, please note that this finer step does not increase accuracy, since makes the intensity variation smoother and wider. This is achieved by setting an approximate XY values nearby the range of Z and wavelength chosen by clicking with the cursor on the "SetXAxis" and "SetYAxis" of the TF OSIRIS Inspector panel (Figure 7.2) and introducing the desired XY values, or using the default ones. Then open the menu of the "setupSweepSwinging"[6] by pressing the green bullet that appears when passing the cursor at the end of this banner. Set "init" as Zi, "step" equal to ΔZ, and "nsteps" to N. Then press the banner "runSweepSwinging" (Blue circle of Figure 6.1). A tiny white stripe will begin to oscillate along the banner indicating that the system is waiting for DAS commands to begin syncro between TF tuning and CCD charge shuffling!

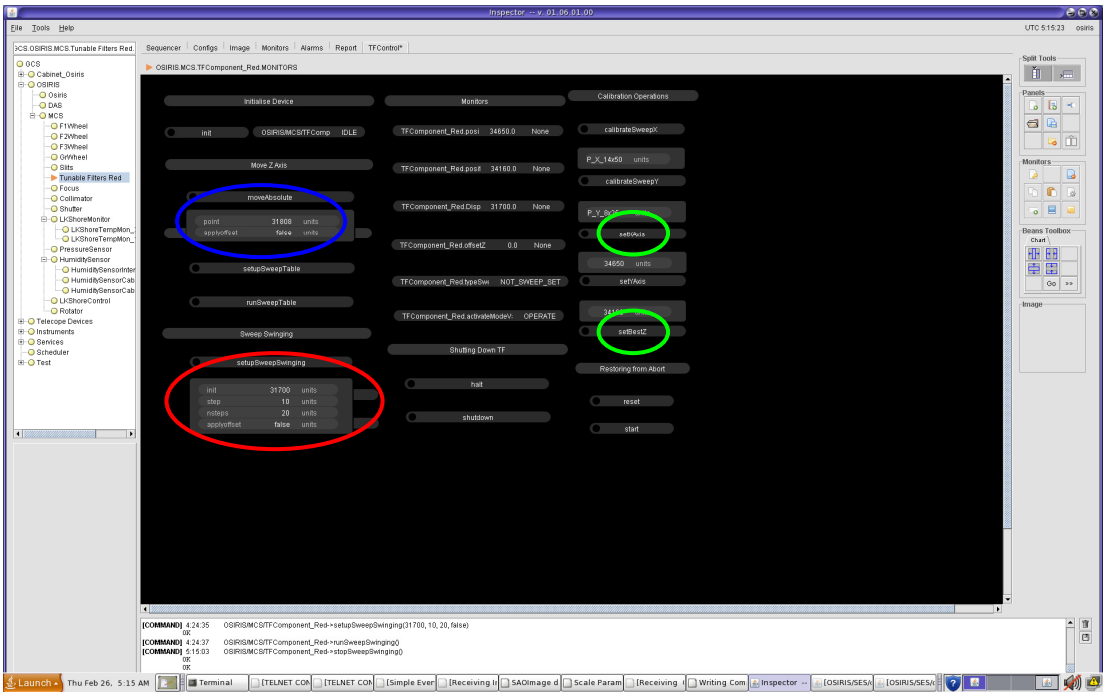

Figure 7.2.- TF control panel from the OSIRIS Inspector. The banners for setting XY are marked in green and the banner for setting up the Z swinging is marked in red.

The following step is programming the OSIRIS DAS (could have been done beforehand leaving it ready just when pressing "expose"). The following parameters have to be changed (Figures 7.3, 7.4 and 7.5):

[6] Sorry for the wizard names.

- On “OPTIONS” flap of the “Data Acquisition System” flap of the OSIRIS “DAS” menu, set a readout speed of 500 kHz to reduce readout time (Figure 7.3)

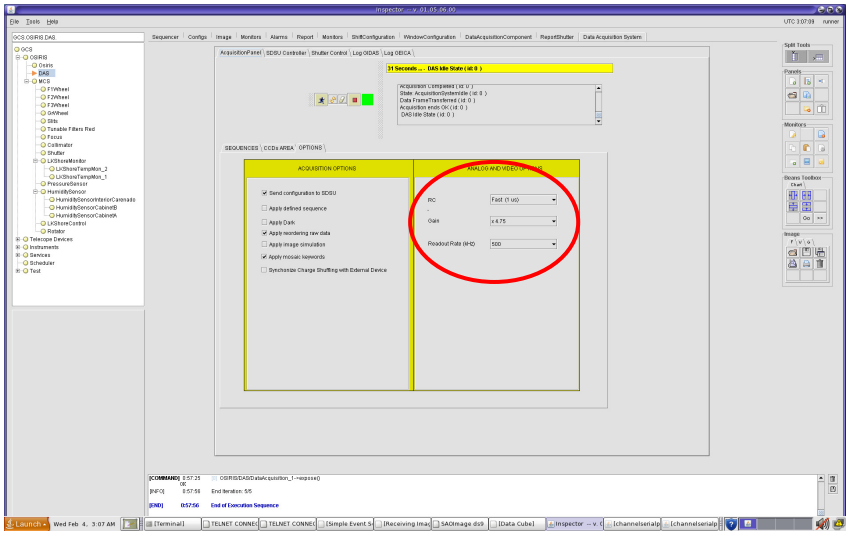

Figure 7.3.- “OPTIONS” flap of the “Data Acquisition System” flap of the OSIRIS “DAS” menu. Set readout speed at 500 kHz and gain 4.75.

- On the “CCDs AREA” flap of “Data Acquisition Window” flap of the OSIRIS “DAS” menu, select CCD1+CCD2-Output A. Do not use split mode (Figure 7.4)

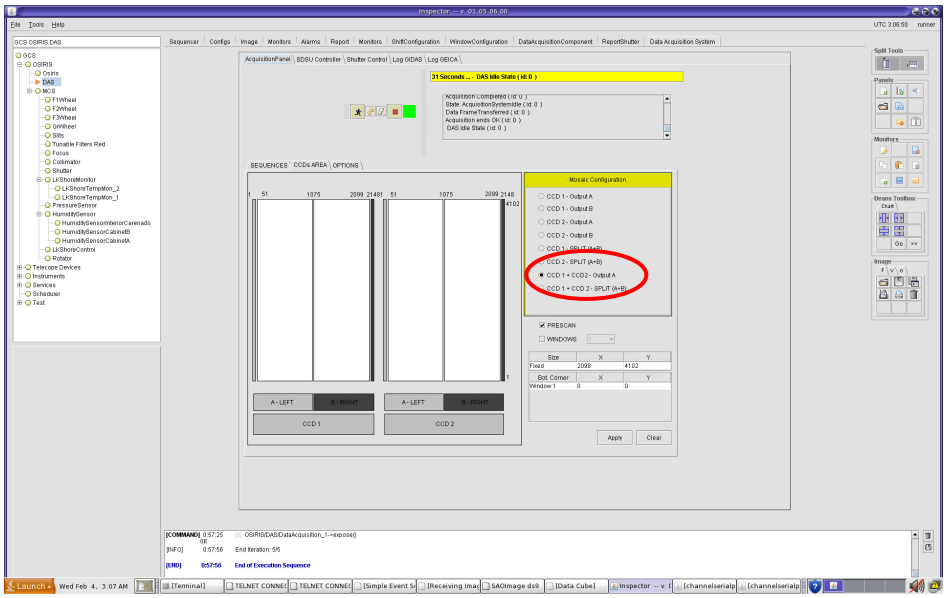

Figure 7.4.- “CCDs AREA” flap of “Data Acquisition Window” flap of the OSIRIS “DAS” menu.

- On the “SEQUENCES” flap of “Data Acquisition Window” flap of the OSIRIS “DAS” menu, choose “Shutterless” exposure type (Figure 7.5, just opens shutter when starting and closes it after the last charge shuffle)

- Set “lines” to 75 (number of lines to shuffle from exposure to exposure). This is enough for not spilling over the detector, but keeping a healthy distance between slit images so that they can be distinguished easily.

- Set “loops” to N

- Set the appropriate exposure time (not smaller than 500 ms)

- Expose by clicking the “running man” icon

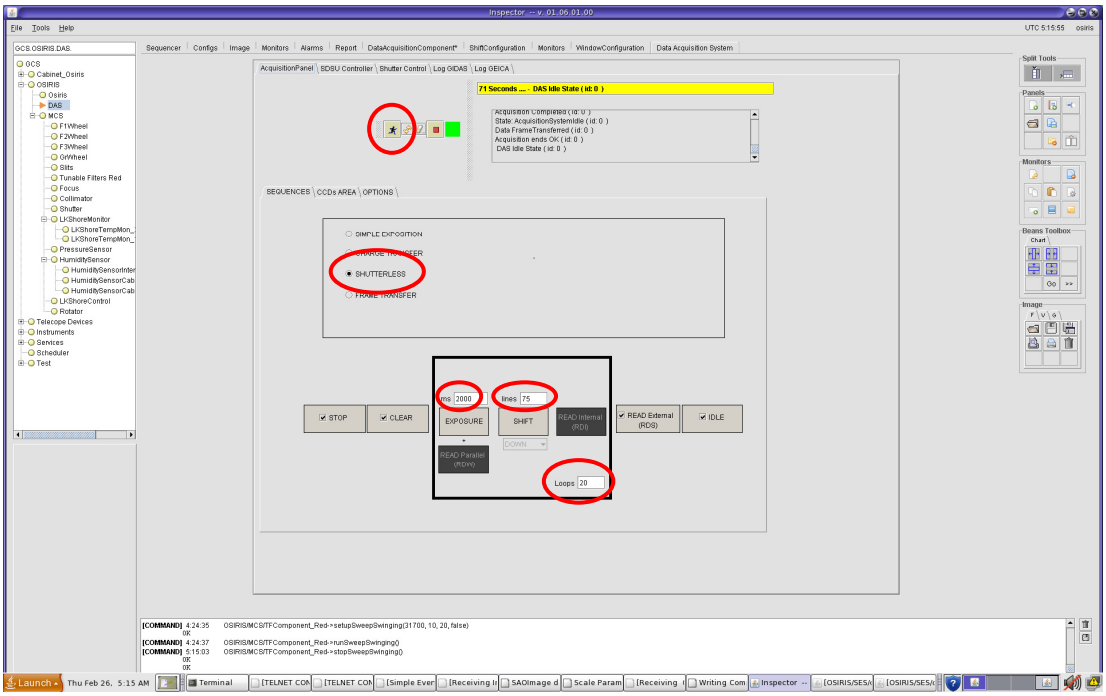

Figure 7.5.- “SEQUENCES” flap of “Data Acquisition Window” flap of the OSIRIS “DAS” menu. The parameters to be set are marked and with the recommended values.

Now OSIRIS is doing the following: programming DAS, clearing CCD, opening shutter, exposing, shuffling charge while changing TF tuning to the next Z by a step ΔZ, and so on. After the last exposure N, it does a last shuffle and closes shutter. When the sequence is finished the TF is kept “Swinging” awaiting for further synchro signal from the DAS and must be stopped by cliking on “stopSweepSwinging” banner of TF Inspector panel (blue circle of Figure 6.1). If any other operation is tried, an error will appear. **The TF cannot be anything else till the swinging is stopped**.

7. Stopped the swinging by cliking on “stopSweepSwinging” banner of TF Inspector panel (blue circle of Figure 6.1)

8. Display the resulting image and search for the brightest slit image either by using the vertical graph of DS9. For this purpose, use *zoom to fit frame*, and *graph vert* from *view* menu. Change scale to adjust to the maximum intensity by changing the maximum using *scale pars* of *scale* menu. Then, use the pixels near the left edge of CCD2 (to give an idea have a look to cursor position in the inset of Figure 7.6), moving the cursor till the

best representative profile is found. Determine the slit image of higher counts, taking into account both peak value and symmetry of the remaining slit images around it. For example, in Figure 7.6 it is clear that the maximum happens between n = 11 and 12. It can be either an exact value or a fraction of step, that can be easily appreciated, yielding the required accuracy of 0.1nm. Alternatively, a fitting program (such as the IRAF routine TFCalibrate.cl, for example) can be used. It has been demonstrated that both procedures are equivalent, of similar accuracy and speed, and that **both require experience**. Please note that the bottom slit image is the first one (initial Z value), and be sure that you have displayed **all** slit images (20 in this case). Simply count the number n of slit images from the first one to the brightest one, both included, and the best Z value will be given by Zbest = [Zi+((n-1) ΔZ)]. Please note that the procedure yields an extra final slit image (i.e. 21 images in this case) with smaller intensity (Figure 7.6). It is produced by a final charge shift and the time elapsed for the shutter to close. Just ignore it.

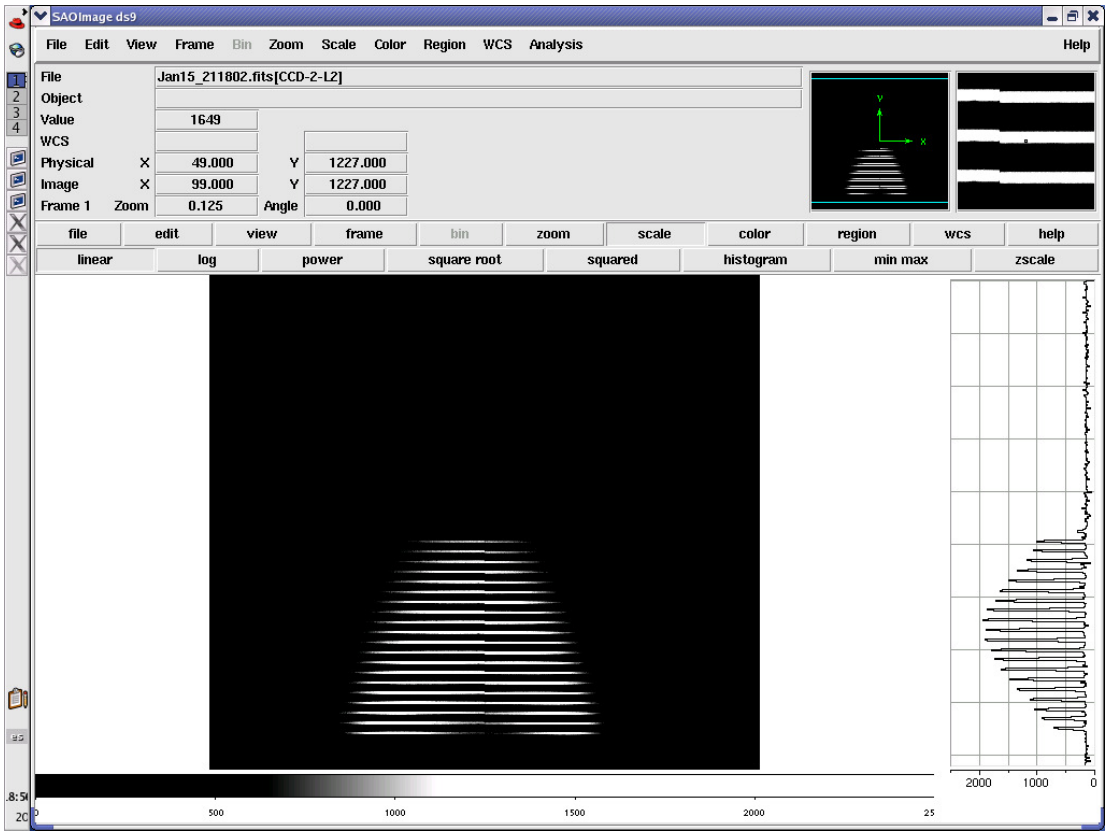
SAOImage ds9
File Edit View Frame Bin Zoom Scale Color Region WCS Analysis Help
File Jan15_211802.fits[CCD-2-L2]
Object
Value 1649
WCS
Physical X 49.000 Y 1227.000
Image X 99.000 Y 1227.000
Frame 1 Zoom 0.125 Angle 0.000
file edit view frame bin zoom scale color region wcs help
linear log power square root squared histogram min max zscale
2000 1000 0
0 500 1000 1500 2000

Figure 7.6.- Z calibration scan. 20 slit images can be seen. The first one is the bottom one. The tuning lies between image 11 and 12 as can be appreciated both from the maximum intensity and symmetry. Non symmetric intensities are suspicious of lack of parallelism. Note the cursor position as shown in the inset image above, and the extra slit image at the end, on the vertical graph. In this case n = 11.5 and then Zbest = Zi + 10.5× 5.

9. **Check that the last value of Z is Zlast = Zi+(N-1) ΔZ (i.e.: the last Z value should be the expected final one minus one step). If not, it means that some steps has been lost (i.e.: Zi is Zi+mΔZ, with typically m=1-3). Correct Zi accordingly based on the Zlast**

provided by Inspector and counting backwards. This should not happen (or rarely) now, but is worth checking.

10. Set Zbest in the TF by inserting the Z value in the "point" deployable menu that appear when cliking on the bullet of "moveAbsolute" banner (blue circle of Figure 7.2) and clicking on the "moveAbsolute" banner to set it. Check that the Z value has changed in the "TFComponent_Red.Displacement". Now the TF is theoretically tuned to the line. But it might be possible that the parallelism is not correct. It will be checked in the next steps using a similar procedure (exposing, shuffling charge but now changing X or Y instead of Z).

11. Take a set of exposures charge shuffling the CCD and varying X from exposure to exposure ±350 bits of the tentative initial value. It is advisable using 14 steps of 50 bit each. In other words: N = 14, ΔX = 50, Xi = X predicted – 350. As in Z procedure, a final extra slit image can appear. This setup is achieved by clicking on the bullet of the "calibrateSweepX" banner. From the deployable menu that appears, choose the option "14x50" (Figure 7.7)

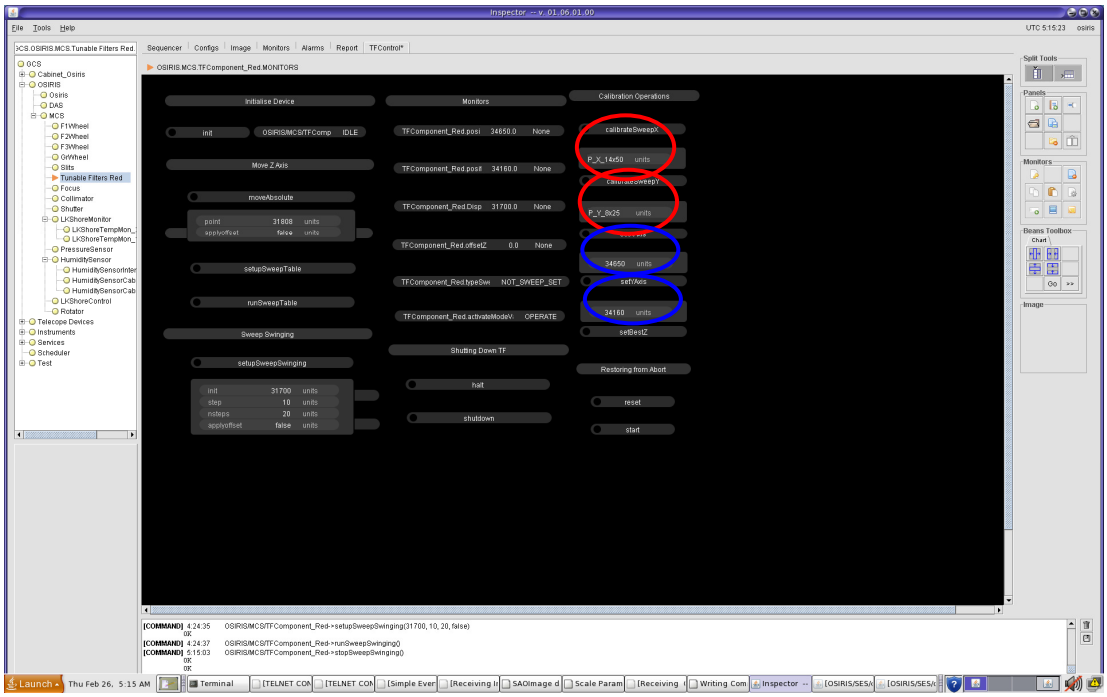

Figure 7.7.- Calibrate X and Y options marked in red on the OSIRIS TF Inspector panel.

12. Please note that the X or Y sweep (contrary to the Z swinging) stops by itself after the programmed number of triggers from DAS. However, **in all cases (X, Y or Z) the user must set the new determined X, Y or Z when finishing the corresponding X, Y or Z calibration sequences** because the TF is left in a value different from the best X, Y or Z value.

13. Check that the last value of X is Xlast = Xi+NΔX (in this case the last value is the last). Otherwise correct accordingly as described for the Z calibration.

14. Look for the brightest slit image as before and calculate Xbest accordingly (Figure 7.8)

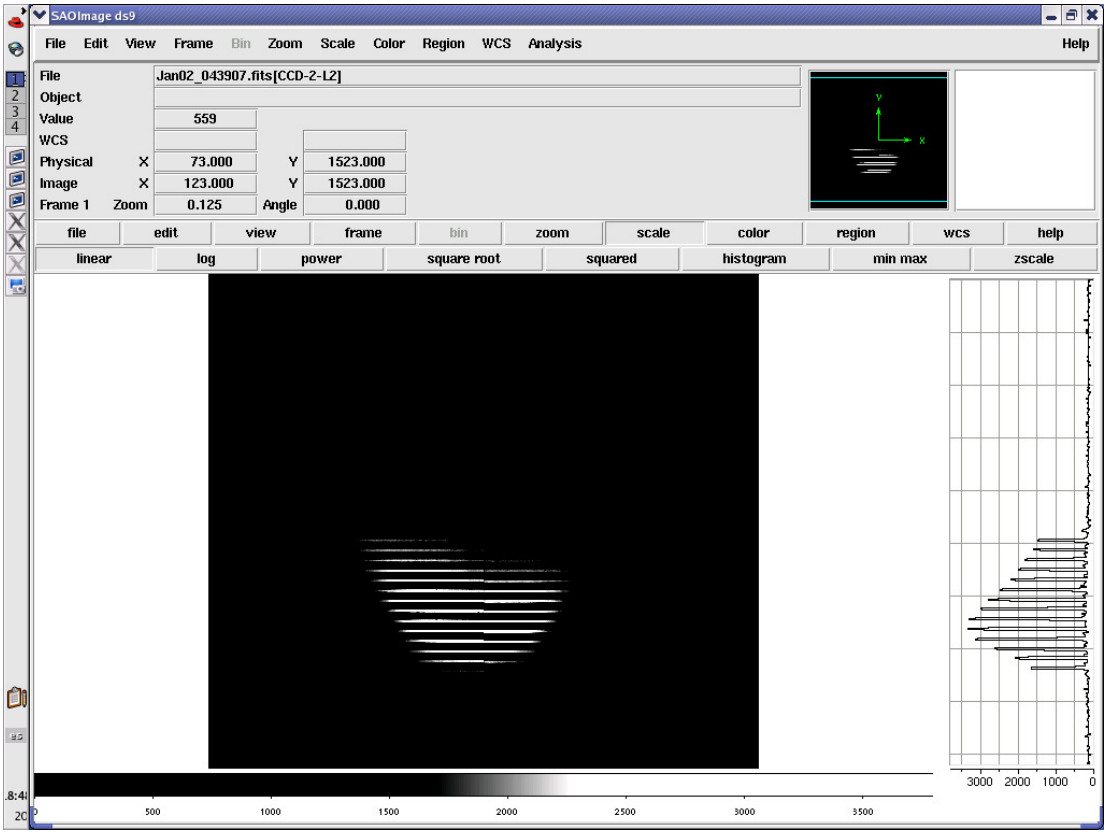
SAOImage ds9
File Edit View Frame Bin Zoom Scale Color Region WCS Analysis Help
File Jan02_043907.fits[CCD-2-L2]
Object
Value 559
WCS
Physical X 73.000 Y 1523.000
Image X 123.000 Y 1523.000
Frame 1 Zoom 0.125 Angle 0.000
file edit view frame bin zoom scale color region wcs help
linear log power square root squared histogram min max zscale
3000 2000 1000 0
500 1000 1500 2000 2500 3000 3500

Figure 7.8.- Example of a X calibration image of 14 steps of 50 bit. Please note that in the X calibration, the slit image intensities are not symmetric. This is normal. The final spurious slit image can be appreciated in the vertical graph. In this case n ≈5.2 and then Xbest = Xi + 4.2×50.

15. Set Xbest by clicking on the bullet of the "setXAxis" banner, inserting the corresponding value on the deployable menu and clicking on the "setXAxis" banner to set it. Check that the X value of the "TFComponent_Red.positionX" has been updated.

16. Calibrate Z as before, since **changing X or Y might change Z** (not viceversa). Changing in ±50 or Y in ±25 bits should not noticeably affect Z. Since the approximate Z value should be nearby the previous one, a ΔZ = 5 could be used from now on. Please note that approximately this step is equivalent to 0.1nm. In other words: calibrating Z in steps of 5 bits you are calibrating with an accuracy of 0.1nm (the one required).

17. Set Zbest as before

18. Now calibrate Y using a similar procedure as done with X, but now using N = 8, ΔY = 25, Yi = Ypredicted – 100, since Y is more sensitive than X. Again, a final extra slit image can appear.

19. Check that the last value of Y is Ylast = Yi+NΔY (in this case the last value is the last). Otherwise correct accordingly as described for the Z calibration

20. Determine and set Ybest as with X (Figure 7.9)

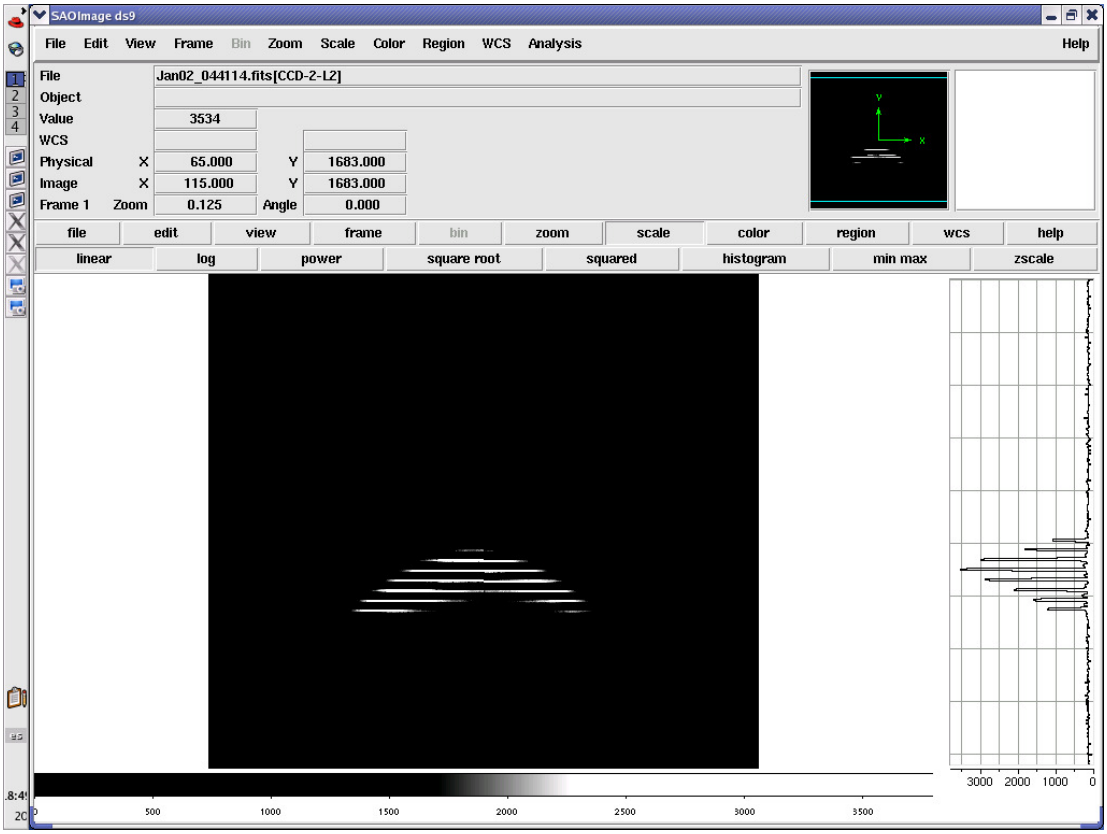
SAOImage ds9
File Edit View Frame Bin Zoom Scale Color Region WCS Analysis Help
File Jan02_044114.fits[CCD-2-L2]
Object
Value 3534
WCS
Physical X 65.000 Y 1683.000
Image X 115.000 Y 1683.000
Frame 1 Zoom 0.125 Angle 0.000
file edit view frame bin zoom scale color region wcs help
linear log power square root squared histogram min max zscale
3000 2000 1000 0
0 500 1000 1500 2000 2500 3000 3500

Figure 7.9.- Example of a Y calibration image of 8 steps of 25 bit. Please note that in the Y calibration, the slit image intensities are not symmetric. This is normal. The final spurious slit image can almost be appreciated in the vertical graph. In this case n ≈5 and then Ybest = Yi + 4×25.

21. Calibrate Z again since changing X or Y might change Z

22. If X and Y were ±50 and ±25, respectively, of the initial tentative values, you have finished. If not, repeat the procedure since changing X (Y) might change Y (X) for achieving parallelism. Once finished, you have XYZ for the required Z range and wavelength. Of course if XY were already known, you can proceed directly to calibrate Z by setting XY and ignoring the previous steps accordingly.

Feel free to repeat any calibration step if you are not confident with the result. Best wasting some time in calibrating than losing much more time throwing your data to the trash after trying painfully to reduce them.

This procedure looks more complicated than it really is. It is more difficult writing the procedure than understanding or executing it. An experienced user can do the previous calibration sequence in few minutes.

NOTE: X is less sensitive to lack of parallelism than Y. Using ΔX=50 and ΔY = 25 with 14 and 8 steps is typically enough. However, be sure that you have the maximum intensity image more or less centred.

7.1.3 Lack of parallelism

A lack of parallelism can be seen as:

- Distorted sky rings
- Asymmetric wavelength calibration (Z) scans, that are in opposite directions depending whether there is an excess or lack in X or Y values (see figure 7.10)
- Lower intensities of slit images in wavelength calibration (Z) scans
- Wavelength shifts

The main consequences for the data are:

- Transmission losses
- Wider FWHM and distorted spectral response (for a TF in a collimated beam)

The XY resolutions used for parallelism calibration, 50 and 25 bits, respectively, have been chosen as the most convenient. Larger steps are not accurate enough and the XY errors affect wavelength and transmission as shown in the following table (approximate values to serve as demonstration only) for the red TF.

± errors Red TF	**λ shift (nm)**	**$\delta T/T$ (%)**
ΔX=±50	0.1	4
	0.1	4
ΔY=±25	0.3	3
	0.2	0

Then, it is important keeping a good parallelism better than 50 bits in X and 25 in Y. Again, note that Y is more sensitive.

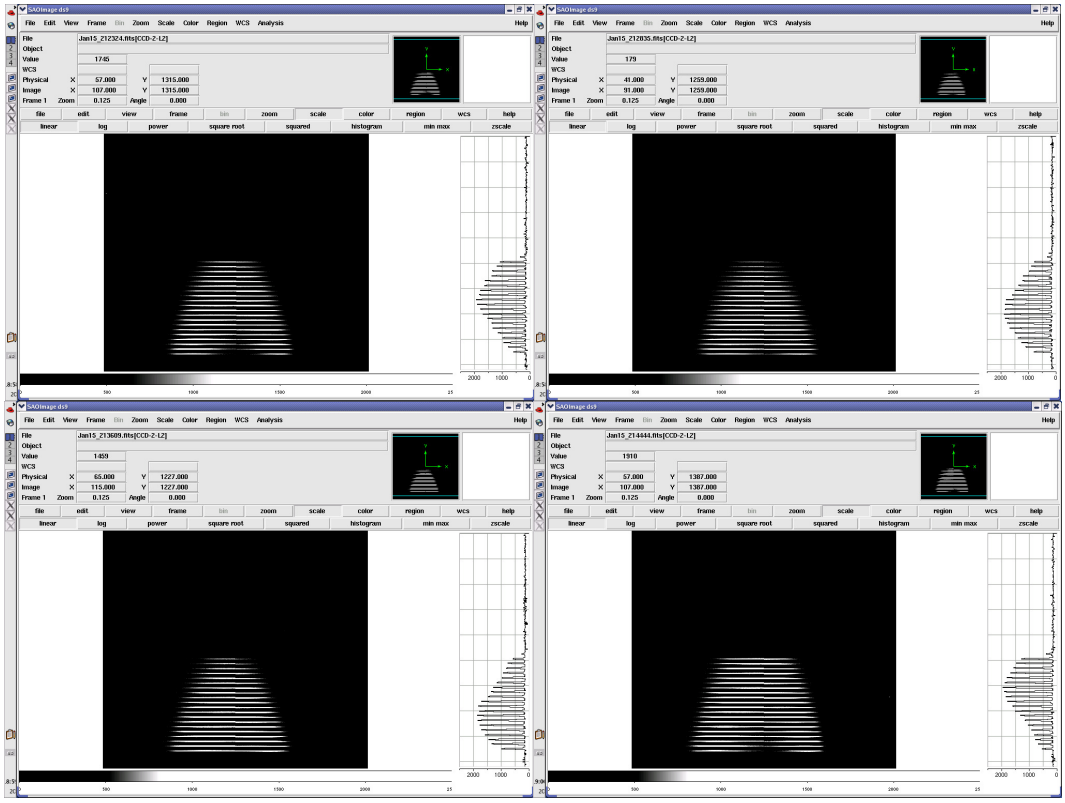

Figure 7.10.- Example of intensity losses and resulting asymmetric slit image intensity profiles obtained for the same Z calibration scan, in the following situations: top-left using Xbest+50 the Z scan is asymmetric and concave **below** the maximum intensity. Top-rigth using Xbest–50 the Z scan is asymmetric and concave **above** the maximum intensity. Bottom-left using Ybest+25 the Z scan is asymmetric and concave **above** the maximum intensity. Bottom-rigth using Ybest–25 the Z scan is asymmetric and concave **below** the maximum intensity.

7.1.4 Troubleshooting

7.1.4.1 The X or Y Sweep does not stop

Likely the system is waiting for more triggers. Check that the number of X or Y Sweeps of the TF is the same as the number of loops in the DAS. To cure it, take another exposure with the number of exposures lacking (or never more, never mind).

7.1.4.2 The X, Y or Z give very different values in consecutive exposures or even mirrored rings

First of all, check that the number of Z steps or X, Y Sweeps are the same as the number of DAS loops. If this is the case, then what has happened is that pick up noise on the DAS-CS100 line is interpreted as DAS trigger signals by the TF and the Xi, Yi or Zi is not the programmed one but several steps have been added. This usually does not happen in X or Y Sweeps, but is more common in Z Swinging. However, **please note that this problem is supposed to be already cured**.

Check the final X, Y, or Z value by using the low level python commands (stop the Z Swinging first) on the same terminal from which Inspector was started:

- . pythondevelopment (with a dot first, and a blank space)
- cd TunableFilters
- python sendCommandTF.py X, Y or Z (for getting the current X, Y or Z values, respectively)

The correct values should be one step less than the final Z, and the final X or Y in the case of X or Y. The reason is that when the final Z is exposed in the Swinging procedure, the CS100 drives the Z to reversal values. Then, if the Z Swinging has ended successfully, the TF will be left one step less in Z than the final value when stopped. If the value of Z is more than one step backwards from the final value, then the starting value has been shift forward by the same number of extra steps backwards. This allows inferring the correct Zbest from the defective Z Swinging image unless the number of extra steps is too large. This is the reason why "mirrored" images could be observed. This does not happens in X or Y Sweep since the loop is exited when the number of triggers are completed.

Please note that this only affects measures where the CS100 is waiting for triggers coming from the DAS (TF calibrations or shuffles), not when a given X, Y or Z is set manually.

7.2 Wavelength calibration

7.2.1 General considerations

While parallelization is a Day Time procedure, because it is very stable with respect to time, temperature changes and even instrument rotation (although again: parallelism varies with Z and wavelength, specially for the blue etalon), wavelength calibration is a Nightly procedure, since the Z-λ calibration depends upon many factors, as already pointed out in Section 4, and the calibration must be checked during the night, even for the same wavelength and order.

The wavelength calibration consist in establishing the relation between Z values in bits and the wavelength. This relation is non-linear enough, so that a linear approximation can be deemed valid only locally. The principles for OSIRIS wavelength calibration are different, though. In a climatic chamber for minimizing temperature and humidity variation, and at the mean yearly temperature of the observatory, the relation between Z and wavelength has been derived for every order and through the full wavelength range that each TF can cover. This relation is fitted by polynomials and programmed in a java-XML calculator. Temperature, humidity and rotator variations does not change the shape of the Z-λ relation, but only the offset between the value predicted by the calculator and the measured one.

Extensive and detailed measures show that this offset can be considered constant along Z and wavelength, with an accuracy of ±5 in Z (i.e.: better than 0.1nm). Anyway, and for securing calibration it is advisable determining the offset for Z and λ values as near as possible the requested ones. Then, wavelength calibrating the OSIRIS TF consist in determining this

offset. This can be done either using a calibration lamp of the ICM or using astronomical targets.

7.2.2 Calibration using the ICM

The calibration procedure using the ICM has already been described within the parallelization procedure of the previous section. It is worth reminding that an accurate Z can be obtained only after parallelization, i.e.: determining the best XY values for the given range of Z and wavelength.

7.2.3 Calibration using astronomical targets

However, since single and intense lines must be used, and given that it is difficult to have an extensive set of lamps of different species, and that lamps of some elements are not available in pencil beam format (i.e.: Helium), it is sometimes advisable using astronomical objects for wavelength calibration. This objects must fulfil the following:

- Narrow lines (i.e.: FWHM smaller than 1.2nm and no peculiar velocity fields)
- Single lines
- Intense lines (to reduce exposure time)
- Of known Doppler or cosmological shift[7]
- Emission line region very compact

These requirements immediately drive to compact PN as wavelength calibrators. Appendix C.2 provides a selection of the compact and bright PN available from La Palma.

However, PN allow mainly calibrating intense lines such as Hβ and [OIII]λ500.7nm, and perhaps [ArIII]λ713.6nm, and [SIII]λ906.9nm. Other lines can be used as well, but must be analyzed with caution: [OII]λλ372.7nm and [SII]λλ671.6,673.1nm are doublets, and Hα has the nearby [NII]λλ654.8,658.3nm lines (then are useful for smaller FWHM). Also, PN concentrate near the galactic plane. Then, in general, PN are ideal for calibrating TF observations of Galactic targets.

[7] The redshift of a galaxy is NOT a Doppler shift, that of a PN does.

Line	Wavelength (Å)	Comments
[NII]	6548.0	Blended with Hα
Hα	6562.8	Blended with [NII]
[NII]	6583.4	Blended with Hα
[SII]	6716.5	Doublet. [NII] and Hα within OS.
[SII]	6730.8	Doublet. [NII] and Hα within OS.
[ArIII]	7135.8	Only HeIλ7065.3Å within OS. Useful for FWHM det.
[SIII]	9068.9	No other line within OS. Useful for FWHM det.
[SIII]	9531.0	No OS available at this moment

Wavelength of relatively intense PN lines

For extragalactic observations of any line at any redshift, [OIII]λ500.7nm emitted by TypeII QSO might be used (at a expense of one order of magnitude integration times): it is a strong, single line, QSO are quite very well distributed, relatively compact, and with a variety of accurately determined redshifts that place [OIII] almost anywhere beyond 500nm. The line is somewhat wide though (300-500 km/s). A list of selected Type II QSO is provided in Appendix C.3.

The procedure for Z calibration using any compact astronomical target, will consist in placing the object into the 2.5arcsec long slit, near the optical centre of the TF in CCD2, and starting a shuffled sequence varying Z, as for an ICM calibration lamp. The brightest image of the source pinpoints the emission line.

7.2.4 Calibration using sky rings

The OH group produce relatively strong emission lines, specially redwards 700nm. These are a nuisance in broad and narrow band imaging as they are for long slit spectroscopy. However, they happens at precise wavelengths and with definite relative intensities and can be used for calibrating spectra or, as in this case, TF. Since the FOV is fully illuminated by these emission lines, rings are produced. Known the wavelength of the emission line, the radius of the ring, that can be obtained using DS9, provides the central wavelength tuned.

As a rule of thumb, for a wavelength drift lower than 0.1nm, the variation Δr of the ring radius r should be, in the worst case:

$$\frac{\Delta r}{r} \leq 0.02 \tag{7.1}$$

For better accuracy,

$$\frac{\Delta r}{r} \leq \frac{n}{2\Delta\lambda}, \tag{7.2}$$

where n is the number of nm of the allowed drift, and $\Delta\lambda$ is the wavelength variation in nm from the centre of the TF (λ_c) to the ring (Eq. 4.3),

$$\Delta\lambda = -7.9520 \cdot 10^{-4} \lambda_c r^2, \tag{7.3}$$

with the radius *r* in arcminutes.

If the ring radius varies in more than the tolerated value, the Z must be changed. If *r* increases, the Z must decrease and vice versa.

The TF tuning must be set so that the **radius** of the ring is of at least ~1000 pix but smaller than ~1800 pix (the 8 arcminute diameter TF FOV). Use CCD2 for measuring the ring using, for example, DS9 (remember that the gap prevents directly fitting a single ring for both detectors).

An experienced user might use ring radius and the above expressions for fast recalibration without using the ICM. However, it is advisable to use the ICM to avoid errors from a tired and sleepy user.

This procedure has the advantage of not requiring change of telescope pointing or switching autoguider off. Only OS and TF tuning. However, please note that the exposure times required are at least of one minute, and that a intense, single and relatively isolated line must be used, but there are not many fulfilling these requirements. For a good sky line map, the reader is referred to Hanuschik (2003), that can be found on-line at http://www.eso.org/observing/dfo/quality/UVES/pipeline/sky_spectrum.html.

It is advisable using the sky line at 894.35nm with the OS 878/59 at FWHM 1.21nm. The recommended parallelism is of X=34550, Y=34140, and it is recommended tuning the wavelength at 898.2nm for obtaining a ring radius of ~1000 pixels.

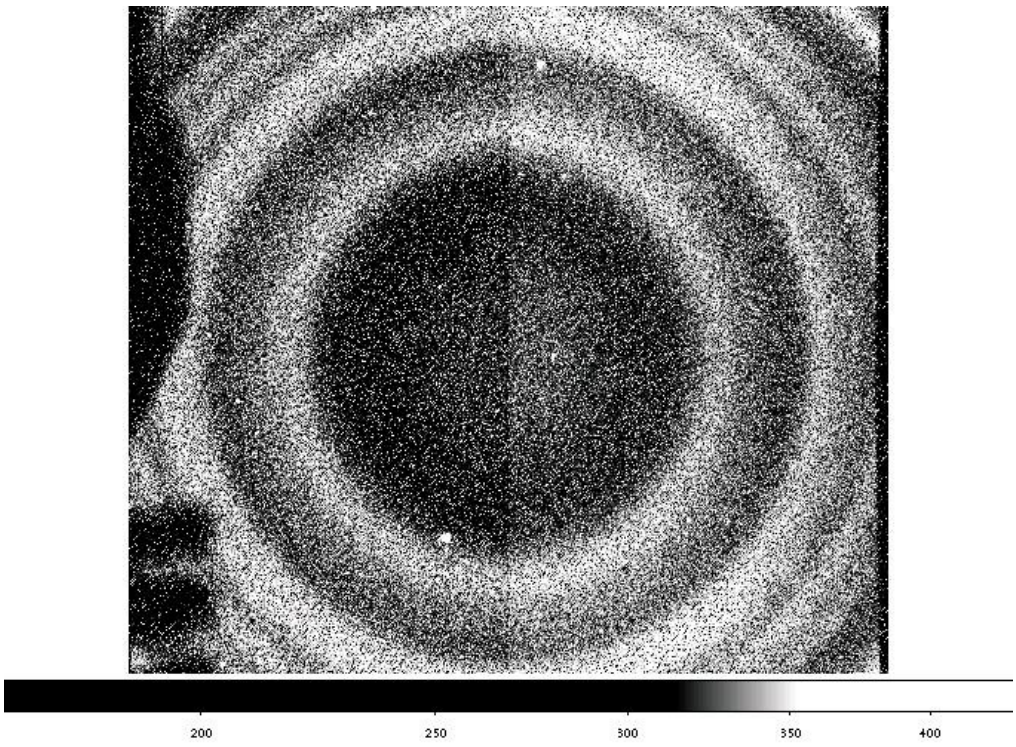

Figure 7.11.- Sky ring at 894.35nm with the OS 878/59 with FWHM 1.21nm, tuning the TF at 898.2nm for obtaining a ring radius of ~1100 pixels. The exposure time is of 120 s.

7.2.5 Trade-offs

Calibrator	Advantages	Disadvantages
ICM lamp	• Short exposure times • No change of telescope pointing required • No need for acquiring target on a slit	• Takes some minutes inserting ICM mirror • During calibration, autoguiding might be lost • Suitable lines not available in some spectral regions
PN	• Provide good zero redshift calibrations • Can be used as flux calibrators for the same price	• Longer exposure times than ICM lamps • Need for acquiring PN on a long slit • Need for change pointing • Some lines are faint • Some lines are not single • Available near Galactic plane
TypeIIQSO	• Calibration can be done almost anywhere on the sky • Calibration can be done almost anywhere on the spectra beyond 500nm.	• Longer exposure times than ICM lamps • Need for acquiring QSO on a long slit • Need for change pointing • The line is fainter than PN • The line is broad
Sky rings	• Does not require changing pointing • Does not require switching autoguider off	• They require at least 60s exposure • Might be tricky to relate ring radius with wavelength. More useful for monitoring than calibration

Trade-off of different TF wavelength calibrators.

We suggest using ICM for wavelength calibration and perhaps sky ring for checking if the calibration is stable and repeating it using ICM if drifting too much.

7.2.6 Measuring TF FWHM

Please note that FWHM (i.e.: TF order) must not be determined using the ICM, since the illumination of the FOV is not representative of that of an astronomical object, and larger values are usually obtained. FWHM can be safely measured using PN. The measures obtained are consistent with those provided by the TF calculator.

7.3 Flux calibration

Using standard spectrophotometric stars as usual using the same settings than for obtaining the data. The STIS Next Generation Spectral Library is recommended.

In the annexes, a list of suitable standards of flat spectra and convenient magnitudes are provided. The full list can be accessed at http://archive.stsci.edu/prepds/stisngsl/datalist.html

8. OPERATING OSIRIS TF

8.1 TF setup

Set the appropriate XYZ as indicated in the calibration procedure (Sec. 7.1.2). XY calibration might be required for new Z and wavelength ranges (to be done during the day, before observations) or set using a table of know XY values versus Z and wavelength. Calibrate Z and determine the offset with respect to the TF calculator. Write down the TF temperature and the temperature gradient in ºC/hour (*LKShore TempMon_2*, number 2. The graph displays the temperature versus time. Change scale accordingly). You are then ready to expose.

There are two possible cases of TF operation:

- Standard tunable imaging, shuffling or fast modes, where exposures at different wavelengths are taken. Wavelength calibration is very critical in this case and special care should be taken.

- Tunable tomography or band synthesis, where a set of exposures at consecutive nearby wavelengths are taken. Wavelength calibration is not so critical in this case[8]. As long as the same reference wavelength for calibration (ICM or PN) is used, although an offset might exists, it would affect equally all images. In other words, images from one day to another will be at the same wavelength although all them might have an offset (the same offset for all of them).

8.2 Standard exposures

Go to “Data Acquisition System” flap of the “DAS” menu. On “CCDs AREA” flap (in the middle of the screen) set the desired readout configuration. On “OPTIONS” flap set the readout speed and gain desired. On the “SEQUENCES” flap set the exposure time in ms. To take an exposure just click on the icon of the running man. The only exposure time that you will use now is “SIMPLE EXPOSITION”

[8] The user must have left some margin as indicated in Secs. 5.6 and 5.7.

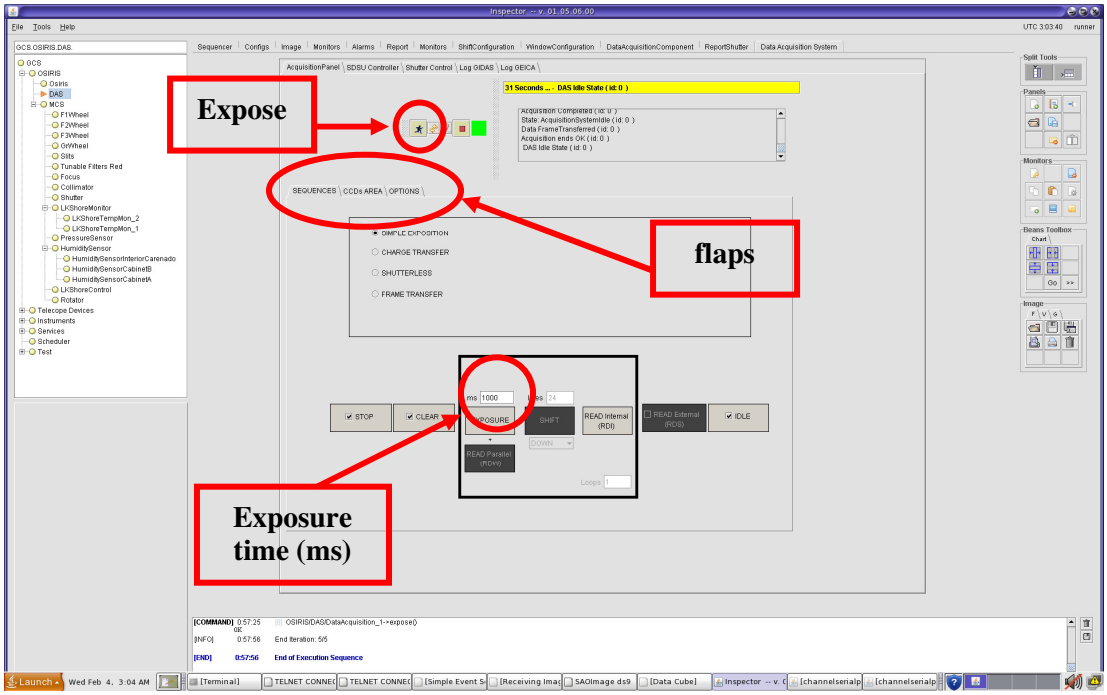

Figure 8.1.- "Data Acquisition System" flap of the OSIRIS "DAS" menu. The running man for exposing, the internal flaps of "SEQUENCES", "CCDs AREA" and "OPTIONS", and the window for setting the exposure time (in ms) can be seen.

Readout configurations of "CCDs AREA" flap (self explanatory, Figure 8.2):

- You can readout only CCD1, only CCD2 or both CCD1+CCD2
- You can readout any of the above using Output A, Output B or both (split mode). I.e.: every CCD has two possible ADCs.

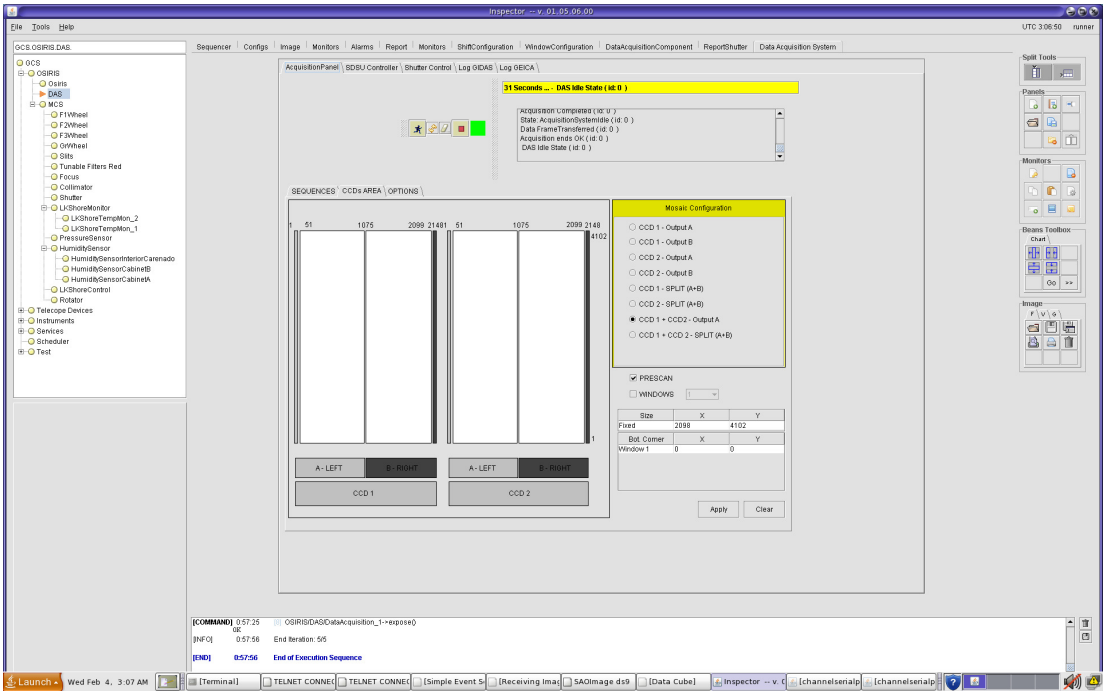
Inspector -- v. 01.05.06.00
File Tools Help
Sequencer Configs Image Monitors Alarms Report Monitors ShiftConfiguration WindowConfiguration DataAcquisitionComponent ReportShutter Data Acquisition System
AcquisitionPanel SDSU Controller Shutter Control Log GIDAS Log GEICA
31 Seconds ... - DAS Idle State (id: 0)
SEQUENCES CCDs AREA OPTIONS
Mosaic Configuration
CCD 1 - Output A
CCD 1 - Output B
CCD 2 - Output A
CCD 2 - Output B
CCD 1 - SPLIT (A+B)
CCD 2 - SPLIT (A+B)
CCD 1 + CCD2 - Output A
CCD 1 + CCD 2 - SPLIT (A+B)
PRESCAN
WINDOWS
A - LEFT
B - RIGHT
CCD 1
CCD 2
Apply
Clear
[INFO] 0:57:56 End Iteration: 5/5
[END] 0:57:56 End of Execution Sequence

Figure 8.2.- "CCDs AREA" flap of "Data Acquisition Window" flap of the OSIRIS "DAS" menu. It is possible to choose the CCD to be read out and the Output (A, B or both) to be used.

Readout speeds of "OPTIONS" flap (Figure 8.3):

- Four slow speeds: 25, 50, 100, 200 kHz, and three fast speeds: 500, 725, 925 kHz are available. Recommended ones are 100 or 200 for imaging. For quick look, acquisition and TF calibration use 500.

If aborting and exposure, the DAS must be initialized again. See troubleshooting section on the OSIRIS USER manual to do that.

Gain of "OPTIONS" flap (Figure 8.3):

- Use 4.75. This is equivalent to ≈1 e^-/ADU

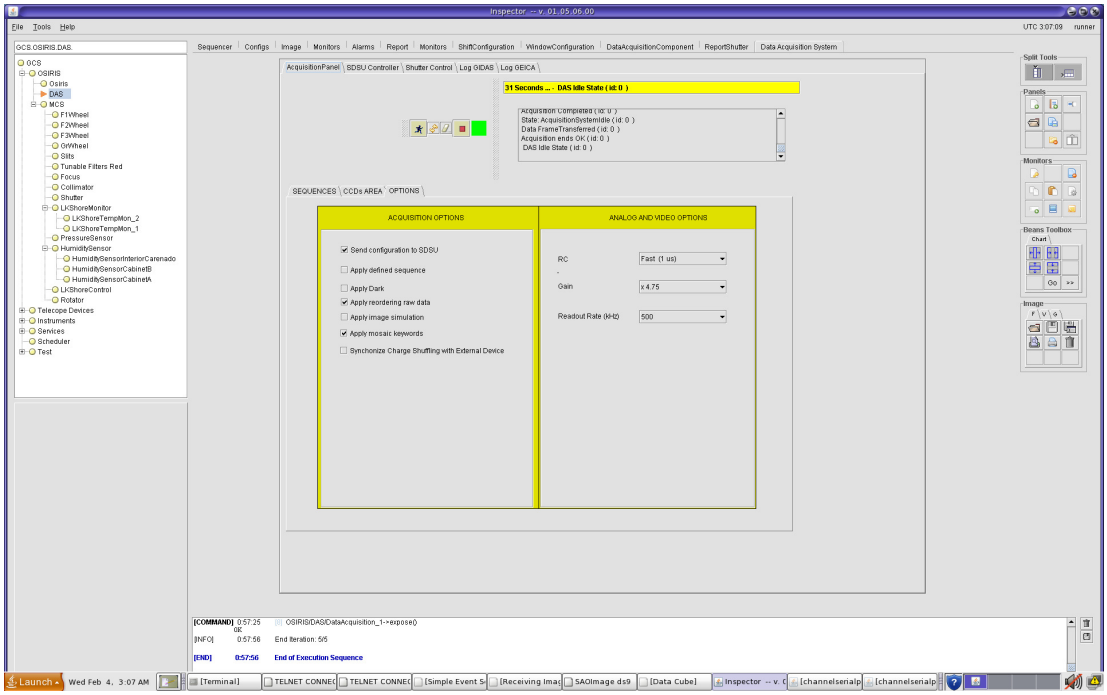

Figure 8.3.- "OPTIONS" flap of the "Data Acquisition System" flap of the OSIRIS "DAS" menu. It allows setting readout speed and gain, and taking bias by ticking on "Apply Dark" option.

Important notes:

1. **Do not abort an exposure unless necessary since the DAS will hang-up** (this problem should be solved by now).

2. **Do not move slits while reading out the CCD**. Otherwise electronic noise appears in the images. However, you CAN move any other mechanism (wheels, collimator, TF) while reading out.

8.3 Shuffled exposures

This section is left for a further version devoted to shuffle and fast modes.

8.4 Fast modes

This section is left for a further version devoted to shuffle and fast modes.

8.4.1 Charge shuffling

8.4.2 Frame transfer

9. OBSERVING WITH OSIRIS TF

9.1 General procedure

The recommended procedure for using a TF is described in this section.

9.1.1 Preparing observation

According to the previous sections, depending on the scientific program, the line to be observed, the type of target, its size, velocity field or velocity dispersion, redshift of Doppler shift, accuracy of this shift, and the number of targets, it is necessary to determine:

- Position of the target(s) in the FOV
- Orientation of the detector on the sky
- Wavelength to be tuned (in the centre of the TF)
- Dithering pattern to be used or use of the half-field mask
- Technique to be used: single exposures, shuffled images, fast photometry, TF tomography or band synthesis
- FWHM to be used. Use calculator for exploring possibilities. This might drive reconsidering the technique to be used if FWHM is too narrow.
- Wavelength range to be scanned (for TF tomography or band synthesis)
- Exposure time
- Use of TF, OS or SDSS filters for continuum subtraction
- The above steps should provide the information required for the OB, including the set of (λ, Z) pairs to be observed

9.1.2 Day time routines

Once selected the required wavelength and Z range for the proposal to be observed during the night, check the LOG for the corresponding XY values. Were XY not available for this pair (λ, Z)[9], it is necessary determining them. For this purpose:

- Choose an emission line from the lamps available at the GTC ICM (see C.1) with a wavelength as near as possible to the line to be observed. Then choose the mode so that the Z is as near as possible the Z required. Use the TF calculator to this purpose
- Insert the ICM and switch the lamp on and the dome lights off
- Insert the 2.5" long slit (specific for tuning the TF)
- With the default XY, scan in Z up and down near the Z provided by the TF calculator till the line is located (Sec. 7.2.2)
- Determine X and Y for this wavelength and Z ranges as described in Sec. 7.1.2, and note it down in the LOG. These values must be logged since XY are very robust and once determined do not need to be determined again

The same line and mode will be used for Z calibration (Sec. 7.2.2)

9.1.3 Practical TF operation and calibrations during the night

- While pointing to the target, insert ICM and switch on the required lamp for Z calibration (see 7.2.2)
- Set XY for the line from the LOG or determined during the day
- Once the telescope is pointing to the target and the rotator angle has been set and stable, avoiding the rotator range from −30º to +60º, perform a Z calibration and note down TF and telescope temperature, TF temperature gradient during the last hour, and the offset in Z units wrt calculator.
- You could use two lines to the blue and red of the required wavelength if desired
- Remove ICM and switch lamp off
- WHILE starting autoguider, tune XYZ for observing an sky calibration ring (see 7.2.4) and write down the ring radius and centre as determined by using DS9 (this is accurate enough as long as you use a reasonable zoom)
- Set the required XYZ to observe the target

---

[9] For the red TF the XY dependence wrt λ and Z is weak. This is not the case for the blue TF. The correction required will be provided by the TF calculator in the future. Meanwhile, this procedure is recommended. Ideally, the wavelength should be within hundred nm and the Z range within few thousand units.

- Expose (see 8.2)

- Every 20-30m check Z calibration observing the sky ring by setting the required XYZ (see 7.2.4). Do not forget to reset XYZ for the target again.

- Recalibrate using ICM if required[10] (wavelength drift larger than the accuracy required)

Please log (see for example E.1 form) wavelength shifts together with TF temperature, TF temperature gradients, TF cabinet relative humidity, and rotator position. This cumulative information will be very useful for implementing future temperature corrections and for further characterizing operation environmental conditions.

10. POST-PROCESSING TF DATA

10.1 General considerations

The TF data reduction procedure is like that of narrow band direct imaging: requires debiassing, flatfielding, combining dithered images (if required), flux calibration using aperture or PSF photometry of spectrophotometric standard stars, and continuum subtraction (if required).

The main differences with narrow band direct imaging are:

- For removing cosmic rays, cosmetics or sky rings, only dithered images at the same tuning (Z) can be combined[11], taking care of the possible wavelength shift of the dithered images, specially at the edges of the TF FOV (see Sec. 5.5 for some hints on alleviating this problem)

- Depending on the type of sources, subtracting continuum images might be unnecessary if a pseudo-spectra is obtained by aperture photometry of the sources observed at different contiguous wavelengths (Sec. 5.7.2)

- Images of the same field at different contiguous wavelengths can be combined in the band synthesis technique (Sec. 5.7)

- In the red spectral domain, instead of fringing, sky rings appear (see 10.3).

[10] An experienced user might use the ring radius to this purpose, thus saving the few minutes required for using the ICM and restarting the autoguider.

[11] As images obtained using different conventional filters would not be combined for this purpose either.

10.2 Calibration images

10.2.1 Bias

Bias shall be obtained and applied as usual. Same readout speed and binning must be selected. See OSIRIS User Manual for the procedure to obtain bias.

10.2.2 Flatfields

Likely due to the non-uniform illumination of the dome, dome flats are not useful unless the target to be analyzed is relatively small (i.e.: the flat is used to correct for small scale variations). Otherwise, sky flats must be then obtained using the same observing parameters (approximate TF tuning and same OS). This is, of course a limitation in the number of wavelengths to be observed each night, but please take into account that, in TF scanning, unless the wavelength range to be covered is very large, or is required changing OS, the same flatfield can be used[12], and that continuing a scan another day is acceptable as long as the same wavelength calibrator is used (see Sec. 8.1).

10.3 Sky rings

The OH atmospheric emission lines are observed through the TF as rings (Figure 7.11), due to its centre to edge wavelength variation. They are equivalent to the fringing observed in direct broad band imaging and, like it, are an **additive** effect. They increase the background photon noise in the zones affected by the ring, thus reducing the S/N in these zones.

Sky rings not necessarily require correcting as long as the ring is not on the target, and the target is not too faint. Nevertheless, if a correction is required, there are several ways to proceed:

- If the targets are not very large, a superflat with the sky ring pattern can be obtained by combination of dithered and smoothed images, even of different pointings: (i) smoothing the dithered images to be corrected using a kernel that wipes small scale structures (sources) but keeps large scale structures (the rings), (ii) obtain the media of the combined smoothed **unmatched** dithered images using a rejection algorithm (the sources are not in the same position due to the dithering, but the rings does since their position depend on the wavelength tuned only). Even images of different pointings can be used as long as the wavelength tuned is the same. (iii) Subtracting the resulting superflat from the original images.

- Running, for example, SExtractor to remove sources thus creating again a superflat.

- Using specially devised programs for creating a synthetic ring image by fitting an azimuthal average of the image, and subtracting it

- Fitting a 2D surface to the ring, creating a synthetic ring image, and subtracting it

[12] In other words: if observing a nearby wavelength with the same OS, the same flatfield can be used.

Needless to say, synthetic ring images does not introduce photon noise in the final image, as the other methods does.

Some of these programs are available in the off-line python pipeline devised by the instrument team and described in the OSIRIS User Manual.

11. POWERING DOWN

¡¡¡YOU MUST NEVER EVER POWER-OFF OSIRIS IF THE TF HAVE BEEN INITIALIZED AND NOT SHUTTED DOWN (I.E.: if in the "IDLE" status). YOU CAN DAMAGE THE TF!!!

- On the Inspector TF menu (Figure 6.1) click on "Halt" and wait till the command has been executed

- Then click on "Shutdown" (Figure 6.1) and wait till the command has been executed (takes three seconds)

Please note: After shutdown the TF cannot be operated again unless you click on "Start" first to put the TF in "ON" status (Figure 6.1).

12. TROUBLESHOOTING

12.1 LCU freezes

If LCU PORT 1 (the one that controls TFs) **freezes while using the TF or with the TF initialized, and you have to initialize it, either by using Crate_27 "switchOff" or by going to the electronic Cabinet-A and using the LCU switch, once the system is recovered, you must first "init" the TF and then first "halt" and after "shutdown" (at Inspector). After that, you can either proceed with the observations or initializing everything again.** Resetting LCUs do not send commands to the TF, then it is safe initializing LCU PORT1 while TF in operation, but then the TFs would be left in the same status forever unless they are initialized again. This is not convenient, and in addition, there is risk of switching off power with the TF in operation or initialized, and this can damage the device.

12.2 TF cannot be shutdown

If you cannot halt and shutdown the TF using Inspector, do not panic (yet). Try closing and opening inspector and giving cntrl-6. If this does not work, go to the terminal used to start Inspector and type:

- . pythondevelopment (with a dot first, and a blank space)

- cd TunableFilters

- python haltTF.py
- python shutdownTF.py

If this does not work. It is likely that either

1. Common services are down and you do not have communication with the TF. In this case the CS most be initialized first. Then "halt" and "shutdown" the TF via Inspector or python commands as described above, before initializing everything again.

2. LCU PORT1 (the one that controls the TFs) is down. This LCU can be initialized **either by using Crate_27 "switchOff" or by going to the electronic Cabinet-A and using the LCU switch**. Resetting LCUs do not send commands to the TF, then it is safe initializing LCU PORT1 while TF in operation, but then the TFs would be left in the same status forever unless they are initialized again. This is not convenient, and in addition, there is risk of switching off power with the TF in operation or initialized, and this can damage the device. To avoid that**, once the system is recovered, you must first "init" the TF and then first "halt" and after "shutdown"** (at Inspector or using python commands)**. After that, you can either proceed with the observations or initialize everything again.**

12.3 TF do not startup

Check whether the TF status (OSIRIS/MCS/TFComp on Figure 6.1) is "ON".

ANNEXES

A. REFERENCES

Atherton et al. 1981, Optical Engineering 20, 806

Atherton P.D. 1995, ASP Conf. Ser. 71, 50

Castro F.J. et al. 2007, *Optical Data of GTC*, RPT/OPTI/nnnn-R

Cepa et al. 2009, *OSIRIS User Manual* (IAC code pending)

González J.J. et al. 2012, SPIE

Hanuschik, R.W. 2003, A&A 407, 1157

Hicks et al. 1984, J. Phys. E. 17, 49

Jones R.V. & Richards J.C.S. 1973, J. Phys. E. 6, 589

SESO 2006, Collimator Unit Measurement Report

Veilleux S. et al. 2010, AJ 139, 145

B. OSIRIS ORDER SORTERS

B.1. Red etalon OSs

λ (nm)	FWHM (nm)	TF λ range (nm)
643.1	27.7	646.2-651.6
648.4	27.9	651.6-657.0
657.2	35.0	657.0-667.6
666.8	35.5	667.6-677.4
680.2	43.2	677.4-692.7
694.4	44.0	692.7-707.1
708.8	44.9	707.1-721.8
723.3	45.2	721.8-736.4
738.0	46.1	736.4-751.3
754.2	49.6	751.3-768.5
770.6	49.7	768.5-784.9
785.6	47.6	784.9-799.4
802.0	51.3	799.4-816.8
819.0	52.4	816.8-834.1
838.6	57.8	834.1-854.9
858.2	57.9	854.9-874.7
878.2	59.3	874.7-895.1
893.2	49.6	895.1-907.9
902.4	40.1	907.9-914.7
910.6	40.5	914.7-923.0
918.9	40.8	923.0-931.5
923.8	34.2	931.5-934.6
927.9	34.4	934.6-938.7
932.0	34.5	938.7-942.9
936.2	34.7	942.9-947.1
940.3	34.8	947.1-951.2

B.2. Blue etalon OSs

C. OSIRIS TF WAVELENGTH CALIBRATORS

For wavelength calibration, either arc lines or emission line objects can be used.

Arc lines have the advantage that are more evenly distributed, are usually more intense, and can be used during day time operation.

Emission line targets usable for wavelength calibration should:

- Have a good sky coverage
- Be relatively compact
- Have lines of narrow, intense, and precise wavelengths.

Compact PN fulfil some of these **in general**[13], and a list is provided below. However, PN are concentrated near the Galactic plane, and do not have many strong lines evenly or properly distributed. They are usually useful for zero redshift targets.

OSIRIS team considers that for some applications [OIII] in type 2 QSO at different redshifts could be used: they are not very narrow, indeed, but are compact, reasonably intense and, more interesting, located over all extragalactic sky at a variety of redshifts spanning the whole optical wavelength range redwards 500nm. However, the exposure times are typically an order of magnitudes those used for PN.

[13] Beware that some PN have peculiar velocity fields!!! For example: Eskimo.

C.1. Selected arc lines

Lamp	Line (Å)	Order Sorter (λ/Δλ)	Exp. Time (s)	X (bit)	Y (bit)	FWHM (calc)	Order
Ne	6506.5	643/28		—	—	—	
Ne	6598.9	657/35	2	34650	34165	14.0	15
				34675	34170	20.5	10
Ne	6929.5	694/44	1	34675	34185	13.8	14
Hg(Ar)	6965.4	694/44	25	34600	34160	13.9	14
Ne	7032.4	694/44	1	34650	34170	13.9	14
Ne	7173.9	709/45	2	34675	34170	13.5	14
Ne	7245.2	723/45	1	34660	34170	13.2	15
Ne	7438.9	738/46	1			13.5	14
Hg(Ar)	7635.1	754/50		34650	34175	13.5	14
Xe	8231.6	819/52	2	34650	34160	12.1	14
				34650	34180	13.1	13
				34700	34170	15.2	11
Hg(Ar)	8264.5	819/52				12.7	13
Xe	8409.2	838/58	15	34600	34150	13.1	12
Hg(Ar)	8521.4	838/58				12.3	13
Xe	8819.4	878/59	2	34375	34060	12.2	15
Xe	8952.2	893/50	10	34550	34140	12.1	16
Hg(Ar)	9123.0	902/40	30	34575	34125	12.5	18
Xe	9162.5	911/40	6	34610	34150	12.3	18

C.2. Selected compact Planetary Nebulae

V84 PN ID	RA J2000 (h:m:s)	Dec J2000 (d:m:s)	Size (arcsec)	Flux Hβ (10^{-13} erg cm^{-2} s^{-1})	Vel. (km/s)	ΔV (km/s)	Comments
153.7–01.4	04 15 54.57	+48 49 40.8	2.0	0.06	—	—	Too faint
184.0–02.1	05 46 50.01	+24 22 02.7	2.0	8.91	+37.4	5.0	
184.6+00.6	05 58 45.34	+25 18 44.0	1.8	0.32	+26.9	—	It's the Southern object
226.7+05.6	07 37 18.91	–09 38 48.1	3.0	9.55	+49.0	10.0	
228.8+05.3	07 40 22.20	–11 32 30.1	3.0	7.59	+100.0	5.0	
049.3+88.1	12 59 27.61	+27 38 14.1	2.7	5.37	–141.0	11.0	
061.9+41.3	16 40 18.14	+38 42 20.1	0.6	26.91			
043.3+11.6	18 27 48.26	+14 29 07.4	1.0	14.79	–6.0	13.5	
051.4+09.6	18 49 47.55	+20 50 39.4	2.6	158.49	+14.0	9.5	
027.6–09.6	19 16 28.22	–09 02 36.6	2.0	45.71	+151	13.1	
042.9–06.9	19 34 33.53	+05 41 02.5	2.0	33.11	–67.7	13.0	
055.1–01.8	19 40 25.18	+18 49 18.8	2.8	0.06			Too faint
082.5+11.3	19 49 46.57	+48 57 40.2	2.0	56.23	–108.8	13.0	
058.3–10.9	20 20 08.76	+16 43 53.3	1.6	295.12	–66.2	14.5	
065.0–27.3	21 29 59.42	+12 10 26.5	1.0	7.94	–140.6		
089.8–05.1	21 32 30.95	+44 35 47.7	1.2	42.66	–26.1	16.5	
111.8–02.8	23 26 14.83	+58 10 54.7	1.0	104.71	–5.0	14.0	

C.3. Selected bright type II QSO

RA J2000 (h:m:s)	Dec J2000 (d:m:s)	Redshift	[OIII] (Å)	Flux [OIII][1] (10^{-16} erg cm^{-2} s^{-1})	EW[OIII] (Å)	Comments
00 25 31.46	−10 40 22.2	0.30349	6523.9	71.1	59	
00 50 09.81	−00 39 00.6	0.72760	8656.8	142.0	281	
00 56 21.72	+00 32 35.8	0.48400	7430.1	124.0	303	
01 14 29.61	+00 00 36.7	0.389	6954.4	33.8	39	
01 20 32.21	−00 55 02.0	0.601	8015.9	49.8	309	
01 23 41.47	+00 44 35.9	0.399	7004.5	94.0	379	
01 34 16.34	+00 14 13.6	0.555	7785.6	107.3	457	
01 42 37.49	+14 41 17.9	0.389	6954.4	42.6	52	
01 49 32.53	−00 48 03.7	0.566	7840.6	69.2	228	
01 57 16.92	−00 53 04.8	0.422	7119.7	202.0	324	
01 59 11.66	+14 39 22.5	0.319	6604.0	42.7	301	
02 10 47.01	−10 01 52.9	0.540	7710.5	208.6	1155	
02 17 57.82	−01 13 24.4	0.375	6884.3	28.6	37	
02 17 58.19	−00 13 02.7	0.343627	6729.1	55.5	95	
02 18 34.42	−00 46 10.3	0.372	6869.3	58.2	66	
02 27 01.23	+01 07 12.3	0.363	6824.3	69.1	89	
02 34 11.77	−07 45 38.4	0.309781	6558.9	74.0	159	
02 49 46.09	+00 10 03.1	0.408001	7049.6	28.2	109	
03 14 49.11	−01 05 02.3	0.557	7795.6	43.3	132	
03 19 50.54	−00 58 50.6	0.626	8141.0	89.9	539	
03 20 29.78	+00 31 53.5	0.3835	6929.4	25.2	35	
03 32 48.50	−00 10 12.3	0.3096	6558.9	39.7	45	
07 37 45.88	+40 21 46.5	0.6137	8076.0	47.4	180	
07 39 10.48	+33 33 53.8	0.4459	7239.8	68.9	353	
07 56 07.16	+46 14 11.5	0.5936	7975.8	27.6	53	
07 57 07.43	+27 36 33.6	0.8189	9102.4	43.6	184	
08 01 54.24	+44 12 34.0	0.5560	7790.6	119.9	1245	
08 12 53.09	+40 18 59.9	0.5513	7765.5	79.1	103	
08 13 30.42	+32 05 06.0	0.3968	6999.5	47.4	78	
08 15 07.42	+43 04 27.2	0.5097	7560.3	144.2	252	
08 40 41.08	+38 38 19.8	0.31309	6573.9	51.2	41	
08 42 34.94	+36 25 03.1	0.5610	7815.6	388.4	881	
08 48 56.58	+01 36 47.8	0.3498	6759.2	34.4	60	
09 02 46.94	+01 20 28.4	0.51326	7575.3	60.7	324	
09 04 14.10	−00 21 44.9	0.3529	6774.2	79.1	92	
09 14 42.33	+00 06 37.2	0.5608	7815.6	41.6	295	
09 20 14.11	+45 31 57.3	0.4022	7019.5	75.0	134	
09 21 52.45	+51 53 48.1	0.5872	7945.8	52.7	199	
09 23 18.06	+01 01 44.8	0.3865	6939.4	65.6	82	
09 23 56.44	+01 20 02.1	0.3796	6909.4	30.4	121	
09 43 12.82	+02 43 25.8	0.5919	7970.8	37.4	232	
09 48 36.05	+00 21 04.6	0.3239	6629.0	37.6	99	
10 27 46.03	+00 32 05.0	0.6136	8079.0	56.9	319	
10 39 51.49	+64 30 04.2	0.4017	7019.5	175.9	304	
10 45 05.39	+56 11 18.4	0.4282	7149.7	70.9	62	

10 48 07.74	+00 55 43.4	0.6427	8221.2	52.1	237	
11 53 14.36	+03 26 58.6	0.5749	7885.7	118.4	238	
11 57 18.35	+60 03 45.6	0.4906	7465.1	169.3	178	
12 26 56.48	+01 31 24.3	0.7320	8671.8	73.8	189	
12 28 45.74	+00 50 18.7	0.5712	7885.7	55.4	293	
12 32 15.81	+02 06 10.0	0.4805	7410.1	219.9	593	
13 23 23.33	−01 59 41.9	0.3503	6759.2	146.8	512	
13 35 50.36	−01 24 39.3	0.5228	7625.4	38.3	75	
13 37 35.02	−01 28 15.7	0.3282	6654.0	57.4	40	
14 07 40.06	+02 17 48.3	0.3092	6553.9	100.5	277	
14 13 15.31	−01 42 21.0	0.3801	6909.4	139.0	339	
14 46 42.29	+01 13 03.0	0.7259	8636.7	38.7	118	
15 01 17.96	+54 55 18.3	0.3386	6699.1	118.0	72	
15 06 08.09	−02 07 44.2	0.4392	7204.8	98.8	685	
15 17 11.47	+03 31 00.2	0.613	8076.0	57.0	545	
15 43 40.02	+49 35 12.6	0.5116	7570.3	51.9	317	
16 41 31.73	+38 58 40.9	0.5959	7990.8	221.7	597	
17 01 51.98	+38 59 01.4	0.5962	7990.8	32.8	187	
17 15 59.79	+28 07 16.8	0.5237	7630.4	53.8	220	
17 26 03.09	+60 21 15.7	0.33340	6674.1	39.5	155	
22 51 02.40	−00 04 59.9	0.550	7760.5	43.7	455	
22 56 12.18	−01 05 08.1	0.648	8251.2	28.7	182	
23 12 39.40	−00 50 05.5	0.479	7405.1	53.0	486	
23 58 18.87	−00 09 19.5	0.4022	7019.5	143.0	195	
23 58 31.16	−00 22 26.5	0.628	8151.1	214.0	676	

Adapted from Zakamska et al. 2003, AJ 126, 2125.
Redshifts from NED database
[1]Assuming a concordance cosmology: H_0=71 km/s/Mpc, Ω_{m0}=0.3, $\Omega_{\Lambda 0}$=0.7.
Typical line widths of 400-500 km/s. Hβ is much fainter, but beware of confusing with nearby [OIII]λ4958.9 , which is about 3 times fainter.
Suggested exposure times are of about 10 s for fluxes 10^{-12} erg cm^{-2} s^{-1}

D. SELECTED STANDARDS FOR FLUX CALIBRATION

E. SOME USEFUL FORMS

E.1. For keeping track of parallelisms and Z offsets

Lamp	Line (Å)	Order Sorter (λ/Δλ)	Exp. Time (s)	X (bit)	Y (bit)	Z (bit)	FWHM (A)	Z (calc) (bit)	FWHM (calc)	Order	Offset Z-Zcal	TF T (ºC)	Hour (hh:mm)	Comments (∇T_{TF})
Ne	6506.5	643/28		—	—		—	—	—					
Ne	6598.9	657/35	2	34650	34165			29876	14.0	15				
				34675	34170			40946	20.5	10				
Ne	6929.5	694/44	1	34675	34185			30398	13.8	14				
Hg(Ar)	6965.4	694/44	25	34600	34160			30213	13.9	14				
Ne	7032.4	694/44	1	34650	34170			29869	13.9	14				
Ne	7173.9	709/45	2	34675	34170			29141	13.5	14				
Ne	7245.2	723/45	1	34660	34170			28773	13.2	15				
Ne	7438.9	738/46	1					30261	13.5	14				
Hg(Ar)	7635.1	754/50		34650	34175			29304	13.5	14				
Xe	8231.6	819/52	2	34650	34160			31798	12.1	14				
				34650	34180			34559	13.1	13				
				34700	34170			40083	15.2	11				
Hg(Ar)	8264.5	819/52						34417	12.7	13				
Xe	8409.2	838/58	15	34600	34150			39424	13.1	12				
Hg(Ar)	8521.4	838/58						38984	12.3	13				
Xe	8819.4	878/59	2	34375	34060			40662	12.2	15				
Xe	8952.2	893/50	10	34550	34140			40071	12.1	16				

Hg(Ar)	9123.0	902/40	30	34575	34125			39237	12.5	18				
Xe	9162.5	911/40	6	34610	34150			39031	12.3	18				